ERCOFTAC
European Research Community
On Flow, Turbulence And Combustion

14th ERCOFTAC SIG 33 Workshop

Progress in Flow Instability, Transition and Control

Cádiz, Spain, June 15-17, 2022

14th ERCOFTAC SIG 33 Workshop

Progress in Flow Instability, Transition and Control

Cádiz, Spain, June 15-17, 2022

Organisers:

Miguel Fosas de Pando (Univ. Cádiz)
Peter J. Schmid (KAUST)
Ardeshir Hanifi (KTH)

UCA Universidad de Cádiz Consejo Social

KAUST

KTH VETENSKAP OCH KONST

FLOW

Wednesday, June 15				
8:45		Registration		
9:00		Welcome		
9:20	Georgios	Rigas	Symmetry-aware proper orthogonal decomposition	Chair: U. Rist
10:05	Manuel	Lorite-Díez	Global modes competition in the streamwise rotating sphere bifurcation scenario	
10:25	Vishal	Chaugule	Extracting Linear Dynamics of High-Speed Jet Flow Using Dual-PIV Combined with Dynamic Mode Decomposition	
10:45	coffee			
11:15	Jitong	Ding	Nonlinear estimation in channel flow at $Re_\tau = 180$	Chair: T. Sayadi
11:35	Anton	Glazkov	New approaches to direct and adjoint sensitivity calculations for the analysis and optimisation of turbomachinery aeroacoustics	
11:55	Gabriele	Nastro	Low-Reynolds-number flows past NACA 4412 swept wings: global stability and sensivity analyses	
12:15	Tobias	Bölle	Explaining coherent vortex dynamics by combining non-normal receptivity and Brownian motion	
12:35	Aliza	Abraham	Instability of three interlaced helical vortices: application to asymmetric rotor wakes	
12:55	Lunch			
14:25	Jens	Fransson	Current status and recent progress on free-stream turbulence induced boundary-layer transition	Chair: P. Luchini
15:10	José	Faúndez Alarcón	Effects of free-stream turbulence scale on disturbance growth on an airfoil and its relation to optimal disturbances	
15:30	Diego	C. P. Blanco	Input-output analysis of boundary-layer transition due to free-stream turbulence	
15:50	Thomas	Jaroslawski	Linear stability analysis on a laminar separation bubble subjected to freestream turbulence	
16:10	Coffee			
16:40	Valerio	Lupi	Modal stability analysis of toroidal pipe flow approaching zero curvature	Chair: L. Lesshafft
17:00	Simon	Kern	Transient growth in asymptotic pulsating channel flow	
17:20	Miguel	Beneitez	Finite-time stability of an optimal edge trajectory in the Blasius boundary layer	
17:40	Javier	Sierra Ausin	Revisiting the O(2) equivariant steady–Hopf interaction	
18:00	Yves-Marie	Ducimetière	Weakly nonlinear evolution of stochastically driven nonnormal systems.	
18:20	End of the day			
Thursday, June 16				
9:00	Soledad	Le Clainche	Reduced order models combining modal decompositions and machine learning tools	Chair: F. Gallaire
9:45	Alejandro	Quirós Rodríguez	Derivative-free optimization of the flow around an airfoil using a cut cell method based solver	
10:05	Diego	Bonkowski Sierra Audiffred	The Wiener-Hopf method applied to experimental boundary layer control	
10:25	Francesco	Scarano	Near wall turbulence control using circular cavities	
10:45	Coffee			
11:15	Marina	Barahona	Interaction of Tollmien-Schlichting waves with Forward-Facing Steps	Chair: J. Soria
11:35	Francesco	Tocci	DNS of the interaction of crossflow instabilities with forward-facing steps	
11:55	Antoine	Jouin	Collective instability of a flow over streamwise and oblique riblet-like roughnesses	
12:15	Tristan M.	Römer	Experimental investigation of vortex structures induced by a roughness element in a boundary layer	
12:35	Yongxiang	Wu	Rotating wall-normal cylindrical roughness elements induced boundary-layer transition	

12:55	Lunch			
14:25	Flavio	Giannetti	Laminar feedback mechanisms of jet tone generation	Chair: T. Leweke
15:10	Lutz	Lesshafft	Effect of Lewis number on the linear stability of jet flames	
15:30	Athanasios	Margaritis	A computational framework for linear analysis of large-scale n-periodic systems	
15:50	Juan Ángel	Tendero Ventanas	Inviscid linear and nonlinear dynamics of viscosity stratified shear layers of one fluid surrounded by another fluid	
16:10	David	Fabre	Aeroelastic and radiative instabilities on a tensioned mem- brane placed under a free surface	
16:30	Social event			
Friday, June 17				
9:00	Pedro	Paredes	Transition prediction in three-dimensional flows with the harmonic linearized Navier-Stokes equations	Chair: J.-C. Robinet
9:20	Sven	Westerbeek	An efficient harmonic Navier-Stokes solver for non-linear stability problems in complex domains	
9:40	Ricardo	Frantz	NekStab: a complete open-source framework for stability analysis of inhomogeneous steady and time-periodic incompressible flows.	
10:00	Daniel	Bodony	Adjoint-Based Optimal Control of Sharp Interface Multiphase Flows	
10:20	Tomas	Fullana	Adjoint-based optimisation of interfacial flows in the sharp interface limit	
10:40	Coffee			
11:10	Omar	Kamal	Global receptivity analysis: toward physically realizable disturbances in hypersonic boundary layers	Chair: S. Hein
11:30	Arthur	Poulain	Linear sensitivity of a hypersonic boundary layer by Algorithmic Differentiation through the toolbox BROADCAST	
11:50	Ganlin	Lyu	Studies of disturbance growth in transonic boundary layers over complex geometries using embedded DG simulations	
12:10	Bruno	Zebrowski	Theoretical and experimental study of transition in choked nozzles	
12:30	Clément	Caillaud	Linear and non-linear dynamics of hypersonic boundary layer streak instabilities	
12:50	Laura Victoria	Rolandi	Compressibility effects on three-dimensional secondary instabilities in the cylinder periodic wake	
13:10	Lunch			
	End of the conference			

SYMMETRY-AWARE PROPER ORTHOGONAL DECOMPOSITION

Georgios Rigas
Dept. of Aeronautics, Imperial College London, London SW7 2AZ, UK

Proper Orthogonal Decomposition (POD) and its variants have been extensively used in the fluid mechanics community for data-driven deduction of turbulent coherent structures and model reduction. Recent variants include nonlinear versions of POD (nlPOD) employing autoencoders with nonlinear activation functions. Coherent structures can be also deduced from stability analysis of the linearised operator of the Navier-Stokes (global or resolvent modes). In order to achieve quantitative agreement between data-driven and operator driven approaches, the nonlinear terms have to be modelled [1] or resolved [2], rendering the operator-driven approaches extremely challenging.

The nonlinear Navier-Stokes equations, are equivariant under symmetry transformations, leading to invariant solutions that are identical up to a prescribed transformation function (i.e. rotation, translation, reflection). The presence of invariant solutions/structures poses an issue for data-driven reduction techniques, since conventional methods encode them into different regions of the reduced space. This leads to an artificial bloating of the latent space. Additionally, for linear POD, where the focus usually lies in the extraction of the modal shapes to gain an insight into the flow structures, these invariances can morph the modes away from physical structures (i.e they become Fourier modes in periodic directions).

In this talk, we present a novel machine learning embedding in the autoencoder, which uses spatial transformer networks and Siamese networks to account for continuous and discrete symmetries, respectively [3] . The spatial transformer network discovers the optimal shift for the continuous translation or rotation so that invariant samples are aligned in the periodic directions. Similarly, the Siamese networks collapse samples that are invariant under discrete shifts and reflections. Thus, the proposed symmetry-aware autoencoder is invariant to predetermined input transformations dictating the dynamics of the underlying system. This embedding can be employed with both linear and nonlinear reduction methods, which we term symmetry-aware POD (s-POD) and symmetry-aware nlPOD (s-nlPOD).

We will demonstrate the proposed framework for 3 fluid flow problems: Burgers' equation, the simulation of the flow through a step diffuser and the Kolmogorov flow to showcase the capabilities for cases exhibiting only continuous symmetries, only discrete symmetries or a combination of both.

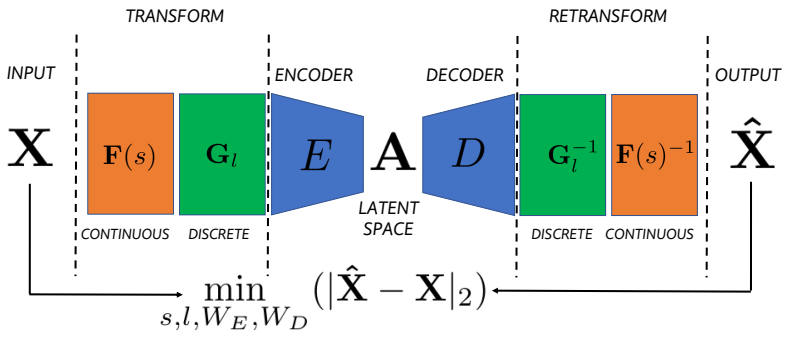

FIGURE 1. *Symmetry-Aware Proper Orthogonal Decomposition using autoencoders*

References

[1] E. Pickering, G. Rigas, O.T. Schmidt, D. Sipp and T. Colonius. Optimal eddy viscosity for resolvent-based models of coherent structures in turbulent jets. *J. Fluid Mech.*, 917, 2021.
[2] G. Rigas, D. Sipp D and T. Colonius. Nonlinear input/output analysis: application to boundary layer transition. *J. Fluid Mech.*, 911, 2021.
[3] S. Kneer, T. Sayadi, D. Sipp, P. Schmid and G. Rigas. Symmetry-Aware Autoencoders: s-PCA and s-nlPCA. *arXiv:2111.02893*, 2021.

GLOBAL MODES COMPETITION IN THE STREAMWISE ROTATING SPHERE BIFURCATION SCENARIO

M. Lorite-Díez[1], J. Sierra-Ausín[2,3], J.I. Jiménez-González[1,4], V. Citro[2], D. Fabre[3]
[1] *Instituto Interuniversitario De Investigación Del Sistema Tierra En Andalucía (IISTA), Universidad de Granada, Universidad de Jaén, Granada 18006 (Spain)*
[2] *Dipartimento di Ingegneria Industriale (DIIN), Università degli Studi di Salerno, Fisciano 84084 (Italy)*
[3] *Institut de Mécanique des Fluides de Toulouse (IMFT), Toulouse 31400 (France)*
[4] *Departamento de Ingeniería Mecánica y Minera, Universidad de Jaén, Jaén 23071 (Spain)*

The wake flow past a streamwise rotating sphere of diameter D, which is a canonical model of many industrial and natural phenomena, is studied here by means of linear stability analysis, normal form analysis and direct numerical simulations to unravel its pattern formation. The problem is governed by two parameters, the rotation rate, Ω (defined as the ratio of the tangential velocity $\omega D/2$ on the sphere surface to the inflow velocity, W_∞) and the Reynolds number, $Re = W_\infty D/\nu$ (where ν is the kinematic viscosity). Our goal is to gain a deeper understanding of the underlying physics and the dominant/fundamental modes of the problem in order to predict the different forces, flow regimes or paths acting on the particle. The performed spatio-temporal characterization helps to understand the complex bifurcation scenario studied by [1, 2] for this configuration and let us evaluate different possibilities of flow and path control. Our systematic study of the mode competition between rotating waves (RW_1, RW_2, RW_3), which are issued from the linearly unstable modes of the steady axisymmetric trivial state (TS), exhibits their connection to previously observed helical (single and double helix) patterns present within the wake. The organizing centre of dynamics turns out to be a triple Hopf bifurcation associated with three non-axisymmetric, oscillating modes with respective azimuthal wavenumbers $m = -1, -1$ and -2 and frequencies LF, MF and HF. The unfolding of the normal form, determined following the method of multiple scales and weakly non-linear analysis, unveils the nonlinear interaction between the rotating waves to constitute more complex states, named as mixed modes (MM_{12}, MM_{13}, MM_{23}). The analysis shows that the transition from the single helix pattern to the double helix structure within the wake displays several regions with hysteric behaviour, which is associated to the existence of multiple attractors (Figure 1a). Eventually, the interaction between single and double helix structures within the wake lead towards temporal chaos, which in this case is attributed to the Ruelle-Takens-Newhouse route. The onset of chaos is detected by the identification of an invariant state of the normal form constituted by three incommensurate frequencies, IMM_{123}. Also, our normal form analysis is complemented with DNS results (Figure 1b) to validate their predictions.

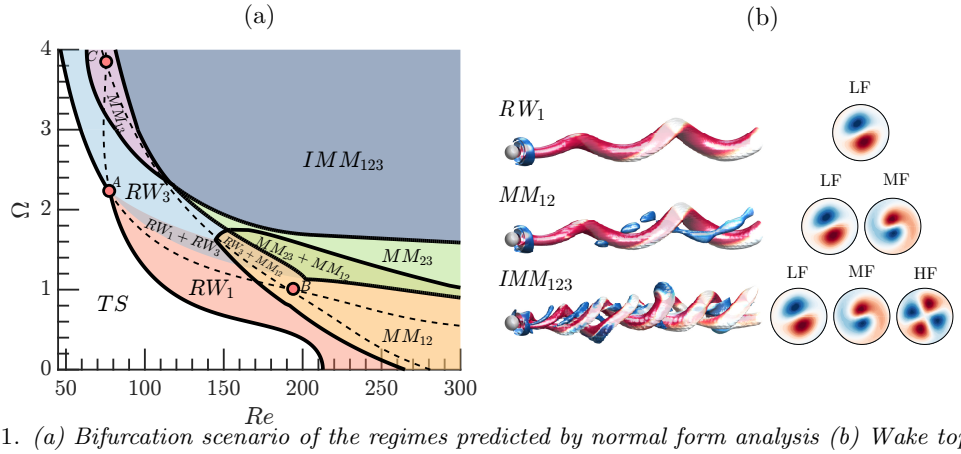

FIGURE 1. *(a) Bifurcation scenario of the regimes predicted by normal form analysis (b) Wake topology and modes for selected regimes at* $\Omega = 1.75$.

This work has been partially financed by the Junta de Andalucía, Universidad de Jaén, and European Funds under Project FEDER-UJA 1262764.

References

[1] M. Lorite-Díez and J. I. Jiménez-González Description of the transitional wake behind a strongly streamwise rotating sphere. *J. Fluid Mech.*, 896: A18, 2020.
[2] B. Pier. Periodic and quasiperiodic vortex shedding in the wake of a rotating sphere *Journal of Fluids and Structures*, 41:43–50, 2013.

EXTRACTING LINEAR DYNAMICS OF HIGH-SPEED JET FLOW USING DUAL-PIV COMBINED WITH DYNAMIC MODE DECOMPOSITION

Alexis Duddridge, Vishal Chaugule, Julio Soria
Laboratory for Turbulence Research in Aerospace and Combustion (LTRAC), Department of Mechanical and Aerospace Engineering, Monash University, Clayton, Victoria 3800, Australia

Due to their importance in propulsion and numerous other industries, free jet flows are a key topic of interest for flow control and manipulation. Understanding of the fundamental processes which lead to instabilities in jets underpins our ability to control them. Numerous studies have utilised particle image velocimetry techniques (PIV) in order to further this understanding but are limited by the time-unresolved data obtained when high spatial resolution is required. These methods are suitable for extracting instantaneous structure and flow statistics but cannot extract the frequencies and corresponding decay, neutral or growth rates of modes or instabilities of the flow. Here, a dual-PIV system is presented, which combined with dynamic mode decomposition (DMD) allows the extraction of the linear shear-layer dynamics of a free jet. The application of this experimental approach coupled with DMD of the acquired dual-PIV dataset allows the extraction of the frequencies of interest and the corresponding spatial modes, which dictate the instabilities in the shear-layer.

The experiments were conducted in the sub/super-sonic jet facility in the Laboratory for Turbulence Research in Aerospace and Combustion (LTRAC) at Monash University. Further details of the experimental rig can be found in [1]. A round jet flow with $Re \approx 10,000$ was the basis for the present investigation. The dual-PIV system consists of a pair of standard single-exposed PIV systems, each receiving oppositely polarized image data via a polarizing beam-splitter from the same imaging optics as shown in figure 1. This polarization approach suggested by Christensen and Adrian (2002) prevents the exposure from one system crossing over to the other. An *Innolas SpitLight DPSS EVO IV dual cavity laser* capable of producing double pulses from each orthogonally polarized cavity on the microsecond scale was utilised to illuminate the central plane of the seeded jet round flow. Two 14 MPx *Imperx-B4820 CCD cameras* separated by a polarizing beam-splitter were used to record the single-exposed PIV image pairs. Timing for the whole system was controlled using a *Beagle Bone Black (BBB)* [3] which sent the appropriate timing signals to each component of the system as dictated by an in-house Python/assembler code. The single exposed PIV image pairs were analysed using an in-house developed parallel multi-grid/multi-pass cross-correlation PIV algorithm, Soria [4].

Using the methodology described in Sikroria et al. [5], the LTRAC sub/super-sonic jet facility was set up for the high-speed subsonic free jet experiment. The challenges associated with extracting temporal information of the small time scales in high-speed jet flows are overcome with the approach described in this paper, allowing key flow structures and their characteristic time scales to be identified. The linear dynamics dictating the instability of the this free shear flow are extracted. The key challenges of utilising a dual-PIV system such as polarization and particle illumination are discussed.

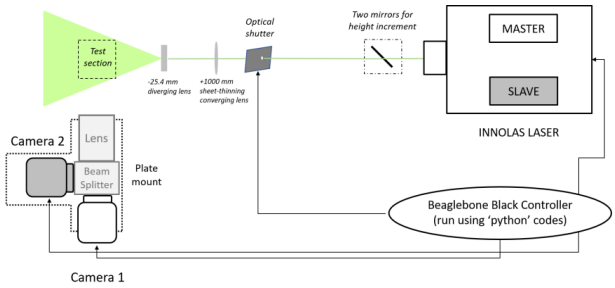

FIGURE 1. *Experimental apparatus and set-up of dual-PIV of a free jet flow at* $Re \approx 10,000$

References

[1] Weightman, J. L., Amili, O., Honnery, D., Edgington-Mitchell, D., and Soria, J. *Nozzle external geometry as a boundary condition for the azimuthal mode selection in an impinging underexpanded jet* Journal of Fluid Mechanics, Vol. 862, 2019, pp. 421–448.

[2] Fedrizzi, Marcus and Soria, Julio *Application of a single-board computer as a low-cost pulse generator* Measurement Science & Technology, Vol. 26(9), 1–4, 2015.

[3] Soria, J. *An investigation of the near wake of a circular cylinder using a video-based digital cross-correlation particle image velocimetry technique.* Experimental Thermal and Fluid Science, 12(2):221–233, 1996.

[4] Sikroria, T., Karami, S., Soria, J., Ooi, A., Sandberg, R. D. *Measurement and analysis of the shear-layer instabilities in supersonic impinging jets using dual-time velocity data* AIAA Aviation 2020 Forum, June 15-19, 2020

NONLINEAR ESTIMATION IN CHANNEL FLOW AT $RE_\tau = 180$

Jitong Ding, Daniel Chung, Simon J. Illingworth
Mechanical Engineering, University of Melbourne, VIC 3010, Australia

This work concerns the estimation problem for a minimal turbulent channel flow at $Re_\tau = 180$ [2] using a reduced-order model. Given the time-resolved velocity information in planes at limited number of wall-normal locations (much less than the DNS grids), how does the estimator yield velocity quantities across the channel height? Below shows the fluctuation velocity equation after the Reynolds decomposition.

$$\frac{\partial u_i}{\partial t} + U_j\frac{\partial u_i}{\partial x_j} + u_j\frac{\partial U_i}{\partial x_j} = -\frac{\partial p}{\partial x_i} + \frac{1}{Re_\tau}\frac{\partial^2 u_i}{\partial x_j \partial x_j} + f_i, \quad f_i = -u_j\frac{\partial u_i}{\partial x_j} + \overline{u_j\frac{\partial u_i}{\partial x_j}} \tag{1}$$

Similar to the work [1], the estimation model is based on the state-space form of the Orr-Sommerfield and Squire equations. The difference is, this time, we calculate the nonlinear forcing terms explicitly and put them as input to the estimator, rather than regard them as unknown white noise. Kalman filter is applied to update the velocity given measurements taken at time interval Δt_1. During Δt_1, a state-space reduced-order simulation is performed at time interval Δt_2 ($\Delta t_2 \ll \Delta t_1$). This simulation only considers large wavenumbers corresponding to large-scale structures which are responsible for a significant fraction of turbulent production, achieving the goal of reduced-order modelling. The state-space model has the form of:

$$x[k+1] = Ax[k] + Bf[k], \quad y[k] = Cx[k] \tag{2}$$

where f is the nonlinear forcing serving as the input; x is the system state containing wall-normal velocity and wall-normal vorticity; y is the output representing the full velocity field.

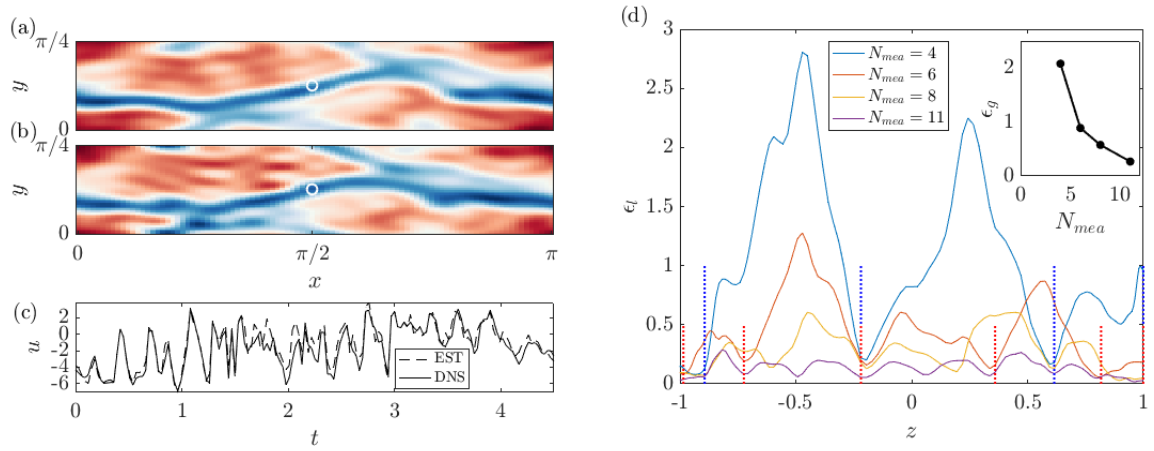

FIGURE 1. *(a): true DNS velocity field; (b): estimated velocity field; (c): results at the white circle in time domain, for the estimation of the streamwise fluctuation velocity at one wall-normal plane. (d): local error versus the wall-normal location for four cases using different number of measurement planes. The inset plot shows the global error versus the number of measurement planes. Vertical dotted lines mark the locations of the measurements for cases $N_{mea} = 4$ (long blue) and $N_{mea} = 6$ (short red).*

Figure 1(a,b,c) shows the results for the estimated streamwise fluctuation velocity at one estimated wall-normal plane (does not coincide with any measurement planes) using 6 measurement planes. Figure 1(d) quantifies the estimation performance by presenting the local error ϵ_l which calculates the difference between the DNS values and the estimation values in the wall-normal direction. The estimator performs better near the measurement planes. Also, the more measurement planes used, the better overall estimation performance will be, as can be seen by the global error curve ϵ_g.

The nonlinear estimator is able to estimate the flow with reasonable accuracy. Further tests have indicated that it does not as yet outperform a simpler, linear estimator augmented with an eddy viscosity [1]. Future work will consider ways to improve its performance and its application to more complex flows.

References

[1] Illingworth, S., Monty, J. & Marusic, I. Estimating large-scale structures in wall turbulence using linear models. *J. Fluid Mech.*. **842** pp. 146-162 (2018)

[2] Chung, D., Monty, J. & Ooi, A. An idealised assessment of Townsend's outer-layer similarity hypothesis for wall turbulence. *J. Fluid Mech.*. **742** (2014)

NEW APPROACHES TO DIRECT AND ADJOINT SENSITIVITY CALCULATIONS FOR THE ANALYSIS AND OPTIMISATION OF TURBOMACHINERY AEROACOUSTICS

Anton Glazkov[1], Peter Schmid[2], Miguel Fosas de Pando[3], Li He[4]
[1] *Postdoctoral researcher at KAUST, Thuwal, Saudi Arabia,*
[2] *KAUST, Thuwal, Saudi Arabia,*
[3] *University of Cadiz, Cadiz, Spain,*
[4] *University of Oxford, Oxford, United Kingdom*

Recent efforts in contemporary turbomachinery design have focused on improving the efficiency of aero engines to address the increasingly demanding regulations for efficiency, emissions of pollutants, and noise. Although many prior efforts have focused on aerodynamic optimisation of turbomachinery blades, the effects of aeroacoustic interactions form self-excited instability processes, complex geometries, and the relative motion between consecutive pairs of rotor and stator blades, remain underexplored and present significant challenges. At the same time, advances in high-performance computing technology are enabling larger and more complex flow calculations, which, with the aid of high-order solvers and adjoint-based methodologies, can be used to attain a granular-level description of the fundamental flow mechanisms in these settings.

This talk presents a novel direct-adjoint framework by means of which such analyses can be carried out in common turbomachinery configurations. The framework is then used to conduct a linear stability analysis for a representative single-passage, subsonic compressor geometry. Here modal and non-modal techniques are used to analyse self-excited instability process within a laminar-separation bubble, at the trailing edge, and within the shear layers on both sides of the blade.

By casting the linear system matrix into block-circulant form, the restriction to single-passage configurations is relaxed to address blade row effects. The modal and non-modal analyses are repeated for a blade row and a comparison to the single passage is highlighted. A preliminary investigation of mistuning effects is also addressed through a perturbation analysis.

The talk concludes by extending this analysis to a rotor-stator configuration, by using a lightweight time-domain sliding plane implementation. Adjoint sensitivities are calculated by making use of nonlinear-adjoint looping, and the results discussed.

The authors gratefully acknowledge financial support from MINECO AEI/ERDF EU Grant No. DPI2016-75777-R, the Alberto Del Vicario Scholarship, EPSRC and the Department of Engineering Science, University of Oxford

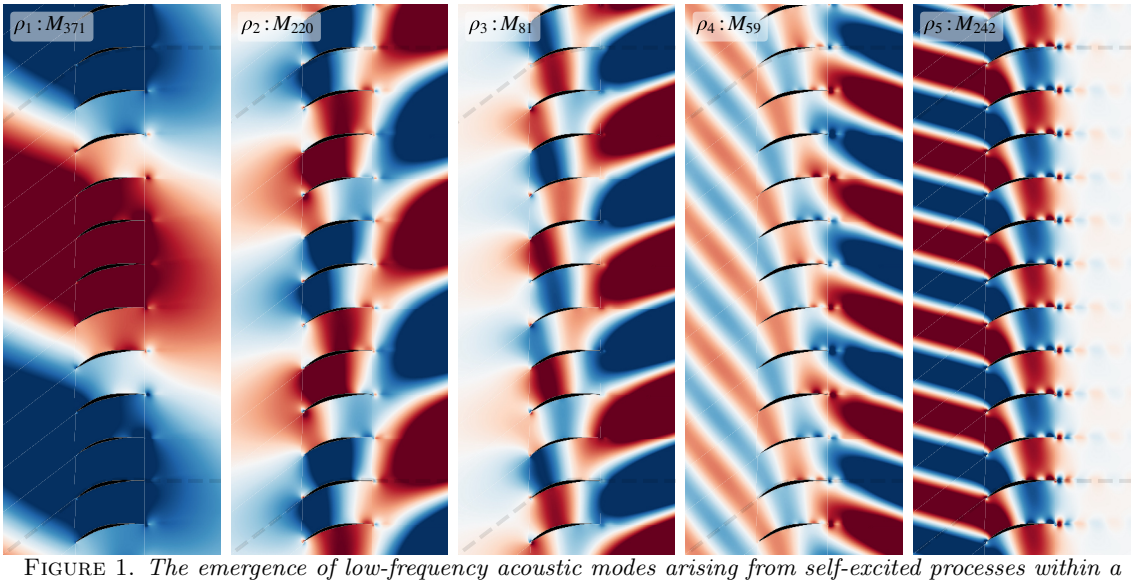

FIGURE 1. *The emergence of low-frequency acoustic modes arising from self-excited processes within a ten-passage blade row.*

LOW-REYNOLDS-NUMBER FLOWS PAST NACA 4412 SWEPT WINGS: GLOBAL STABILITY AND SENSIVITY ANALYSES

G. Nastro[1,2], J.-C. Robinet[2], J.-C. Loiseau[2], P.-Y. Passaggia[1], N. Mazellier[1]
[1] *Laboratoire PRISME, Université d'Orléans, 45072 Orléans Cedex, France*
[2] *Laboratoire DynFluid, Arts et Métiers ParisTech, 75013 Paris Cedex, France*

Global stability and sensitivity analyses of steady spanwise-homogeneous laminar separated flows around periodic NACA 4412 wings with sweep angles between $0° \leq \Lambda \leq 25°$ are numerically performed for different Reynolds numbers and angles of attack.

The wake dynamics is attenuated by increasing Λ and driven by the two-dimensional von Kármán mode (see Figure 1 and Ref. [1]). Its emergence threshold in the $(\alpha - Re)$ plane is computed together with that of the stall mode [2, 3] whose emergence Reynolds number is found to be ~ 1.8 times that of the von Kármán mode. At the critical conditions the Reynolds number, the Strouhal number, the streamwise wavenumber of the von Kármán mode and the spanwise wavenumber of the leading stall mode show a power-law behaviour with respect to α. Introducing a sweep angle entails a Doppler effect in the leading modes' dynamics and a shift towards non-zero frequencies for the stall modes which result to be non-dispersive in the spanwise direction as opposed to the von Kármán modes.

Sensitivity of the leading global modes [4] is investigated in the vicinity of the critical conditions through adjoint-based methods to predict regions of the flow which are most sensitive to the application of steady forces (see Figure 2). As illustrated in Figure 2(a), the growth rate sensitivity function displays an extended region on the wing's suction surface close to the leading edge wherein a streamwise oriented force has a net stabilising effect, comparable to the one inside the recirculation bubble. In accordance with the sensitivity analysis, a localised spanwise-homogeneous force is found to suppress the Hopf bifurcation and stabilise the entire branch of von Kármán modes.

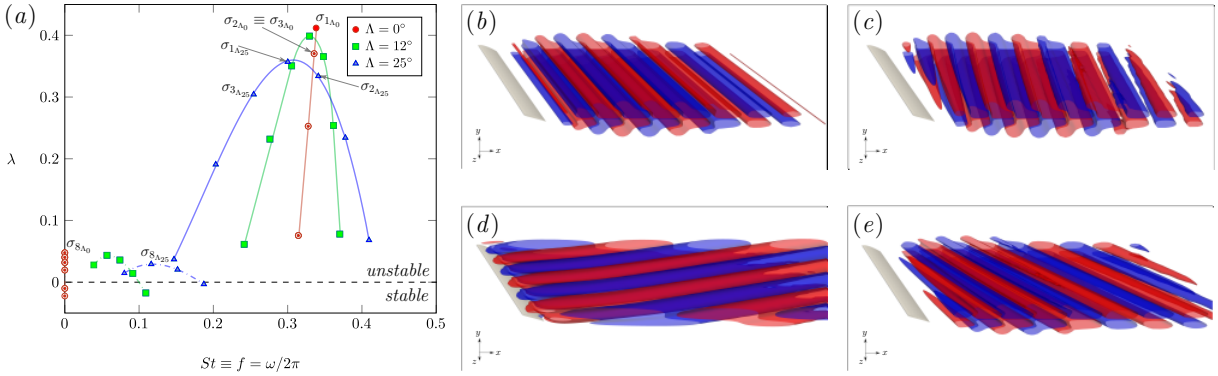

FIGURE 1. *(a) Eigenspectrum for $\Lambda = 0°, 12°, 25°$ at $\alpha = 20°$ and $Re = 400$ and real parts of the streamwise velocity* $\mathrm{Re}(\hat{u})$ *of the eigenfunction corresponding to (b) the two-dimensional von Kármán mode $\sigma_{1_{\Lambda_{25}}}$, (c-e) the three-dimensional von Kármán modes $\sigma_{2_{\Lambda_{25}}}$ and $\sigma_{3_{\Lambda_{25}}}$ and (d) the stall mode $\sigma_{8_{\Lambda_{25}}}$.*

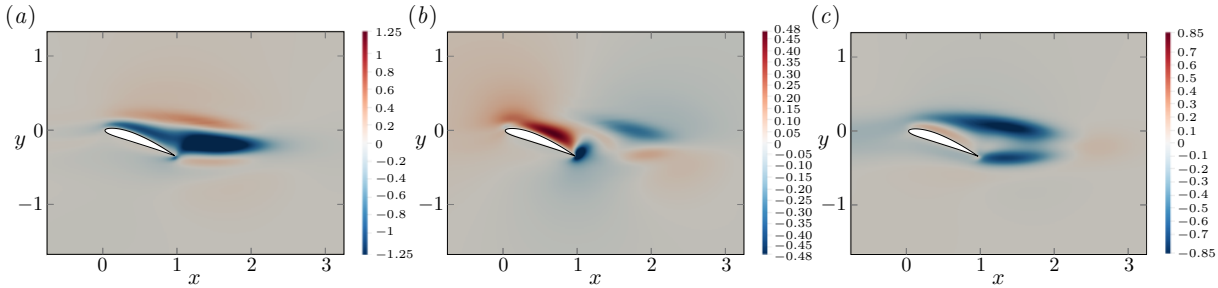

FIGURE 2. *(a) Streamwise, (b) cross-stream and (c) spanwise components of the growth rate sensitivity to a steady force of the leading eigenvalue for $\Lambda = 25°$, $\alpha = 20°$ and $Re = 190$.*

References

[1] W. He, R. S. Gioria, J. M. Pérez and V. Theofilis. Linear instability of low Reynolds number massively separated flow around three NACA airfoils. *J. Fluid Mech.*, 811:701–741, 2017.
[2] V. Kitsios, D. Rodríguez, V. Theofilis, A. Ooi and J. Soria. BiGlobal stability analysis in curvilinear coordinates of massively separated lifting bodies. *J. Comput. Phys.*, 228(19):7181–7196, 2009.
[3] D. Rodríguez and V. Theofilis. On the birth of stall cells on airfoils. *Theor. Comput. Fluid Dyn.*, 25(1):105–117, 2011.
[4] O. Marquet, D. Sipp and L. Jacquin Sensitivity analysis and passive control of cylinder flow. *J. Fluid Mech.*, 615:221–252, 2008.

EXPLAINING COHERENT VORTEX DYNAMICS BY COMBINING NON-NORMAL RECEPTIVITY AND BROWNIAN MOTION

T. Bölle[1]
[1] *Institute of Atmospheric Physics, DLR, Münchener Str. 20, 82234 Wessling, Germany, tobias.boelle@dlr.de*

Coherent vortices are important building blocks of complex flows on all scales. In particular, trailing vortices behind aeroplanes considerably influence contrail formation and flight safety. Robust control strategies, however, require a thorough understanding of the governing dynamics. The main unsteadiness of large-scale vortices in this configuration, being the subject of this study, is called meandering [1]. Despite a common observation in experiments since the 1970s and a multitude of studies, its origin and physical mechanism remain puzzling.

We present the first encompassing theoretical model to explain the phenomenon in all fundamental characteristics. On a scale-separation argument between the (large-scale) vortex and the surrounding (small-scale) turbulence, we show that the vortex response is governed by a Langevin equation of (abstract) Brownian motion. This amounts to a reduced-order model describing the vortex response, driven by a stochastic forcing (Wiener process). In this model, we can readily infer the experimentally, universally observed statistics (see figure 1). We, hence, come to the important conclusion that vortex meandering is a manifestation of a Gauss–Markov process that can be described in the framework of *linear* response theory [2]. This allows us to use results of a study on the non-normal receptivity of canonical vortices [3]. Starting from the premise that non-normality is necessary for receptivity to free-stream disturbances, we explore the non-normality of canonical vortices. In particular, we derive a direct connection between receptivity, critical-layer forcing and non-normality. This prototypical vortex amplification can be understood by an adaptation of the mother–daughter mechanism of [4] as is shown in figure 1.

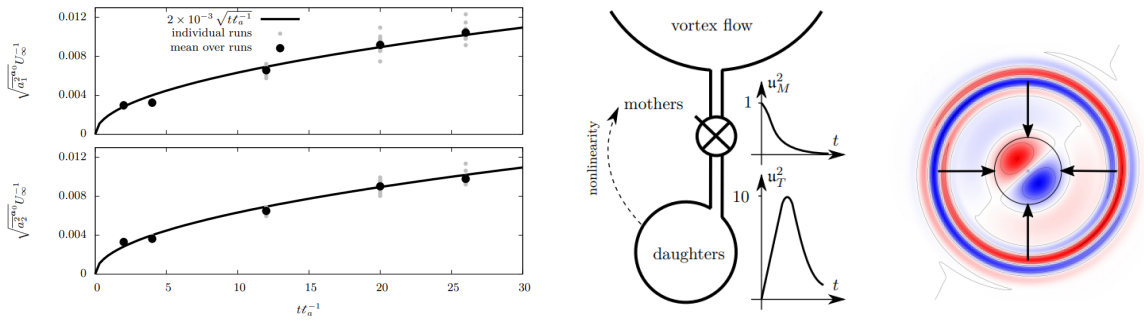

FIGURE 1. *Linear vortex response dynamics. Variance amplification of the analytical reduced-order model compared to experiment (left); mother–daughter mechanism (middle); receptivity prototype from canonical decomposition of the resolvent, showing critical-layer forcing (right).*

Definite evidence for the linearity and low-dimensionality of the large-scale unsteadiness of experimental vortex dynamics can be seen as important results on their own. Moreover, understanding vortex dynamics in terms of linear response theory of a reduced-order model and the mother–daughter mechanism may be used to develop control strategies. It is expected that the proposed theory readily extends to comparable flow configurations.

References

[1] L. Jacquin, D. Fabre, P. Geffroy and E. Coustols. The Properties of a Transport Aircraft Wake in the Extended Fear Field: An experimental study. In: 39th Aerospace Sciences Meeting and Exhibit, 1038, 2001
[2] R. Kubo, M. Toda and N. Hashitsume. *Statistical Physics II: Nonequilibrium Statistical Mechanics*. Springer-Verlag, Berlin, 1998
[3] T. Bölle, V. Brion, J.-C. Robinet, D. Sipp and L. Jacquin. On the linear receptivity of trailing vortices. *Journal of Fluid Mechanics*, 908, 2021
[4] L. Boberg and U. Brosa. Onset of turbulence in a pipe. *Zeitschrift für Naturforschung A*, 43, 697–726, 1988

INSTABILITY OF THREE INTERLACED HELICAL VORTICES: APPLICATION TO ASYMMETRIC ROTOR WAKES

Aliza Abraham[1], Andrés Castillo-Castellanos[1], Thomas Leweke[1]
[1]*IRPHE, Aix-Marseille Université, CNRS, Centrale Marseille, Marseille, France*

Helical vortex filaments are subject to various types of instabilities, including displacement instabilities, which occur when the vortex core is shifted from its baseline position. The theoretical growth rates of unstable displacement perturbation modes have long been established for one helix [1] and multiple interdigitated helices [2], but experimental investigations into the dynamics of helical vortices are scarce. Quaranta et al. [3, 4] experimentally excited different instability modes using one- and two-bladed rotors to generate helical vortices, and found close agreement with theoretical growth rates. The current study investigates the helical vortices in the wake of a three-bladed rotor, focusing on perturbation modes with zero azimuthal wavenumber, which can be triggered by rotor asymmetry.

This instability is explored using water channel experiments, vortex filament simulations and a simplified point-vortex-based model. In the experiments, vortices shed from the tips of a three-bladed rotor with a 9 cm radius are visualized by painting the blade tips with fluorescent dye and illuminating the water channel test section with an LED panel (Figure 1a). The blades are 3D printed and can be removed and replaced individually to introduce different initial perturbations. The simulations monitor the evolution of helical vortex filaments modelled as concentrated material lines of vorticity, as described in [5], with an initial displacement. To provide a tool to explore a wide range of perturbations quickly, a simplified model using a periodic strip of point vortices to represent a cross-section of the helical vortex system is developed. In spite of its simplicity, it is shown to accurately capture the key features of the helical vortex interactions (Figure 1b).

The growth rate and displacement modes obtained using these methods agree well with the theory for the zero-wavenumber perturbations. Results of this study show that the three-helix system is highly sensitive, with small initial perturbations on the order of 5% of the vortex separation distance substantially disturbing the rotor wake within a few turns of the helices (Figure 1). This sensitivity is shown to vary with the direction of the perturbation, with displacements along the positive strain direction developing faster in the non-linear regime than those along the negative strain direction. These findings have applications to industrial flows, such as those found in the wakes of wind turbines, propellers and helicopter rotors, where coherent vortices can induce strong loading on downstream structures. Introducing an asymmetry to these rotors, which represents a means of passive control, could accelerate coherent structure breakdown, mitigating such detrimental wake effects.

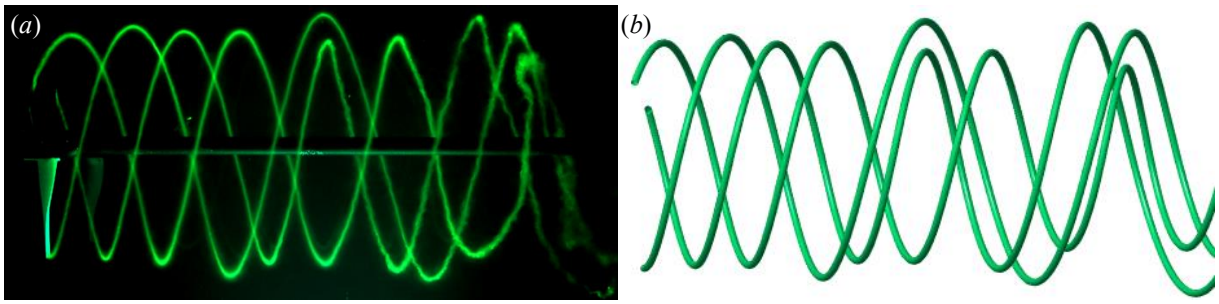

FIGURE 1. *(a) Dye visualization of the helical vortices in the wake of an asymmetric three-bladed rotor. (b) Helical vortices reconstructed from a simplified point vortex model.*

References

[1] S. E. Widnall. The stability of a helical vortex filament. *J. Fluid Mech.*, 54(4):641–663, 1972.
[2] B. P. Gupta and R. G. Loewy. Theoretical analysis of the aerodynamic stability of multiple, interdigitated helical vortices. *AIAA J.*, 12(10):1381-1387, 1974.
[3] H. U. Quaranta, H. Bolnot, and T. Leweke. Long-wave instability of a helical vortex. *J. Fluid Mech.*, 780:687–716, 2015.
[4] H. U. Quaranta, M. Brynjell-Rahkola, T. Leweke, and D. S. Henningson. Local and global pairing instabilities of two interlaced helical vortices. *JJ. Fluid Mech.*, 863:927–955, 2019.
[5] E. Durán Venegas and S. Le Dizès. Generalized helical vortex pairs. *J. Fluid Mech.*, 865:523–545, 2019.

CURRENT STATUS AND RECENT PROGRESS ON FREE-STREAM TURBULENCE INDUCED BOUNDARY-LAYER TRANSITION

Jens H. M. Fransson
Department of Engineering Mechancis, KTH–Royal Institute of Technology, Stockholm, Sweden.

To date, very few careful and direct comparisons between experiments (EXP) and direct numerical simulations (DNS) have been published on free-stream turbulence (FST) induced boundary-layer transition, whilst there exist numerous published works on the comparison of canonical turbulent boundary layers. Quite often computational fluid dynamic (CFD) results are compared to either EXP or DNS, mainly for validation purposes and mostly for fully turbulent flows but where careful comparisons are lacking. Despite discrepancies, these can sometimes be accepted without much thought even though we must be critical and ask ourselves *why* there are deviations. It is first until one can claim that the underlying physics is understood and that the behaviour of the model has been scrutinized in-depth, that one can start discussing possible reasons for the deviations, such as different inlet and background conditions in EXP versus computations. However, to be honest, this type of discussion is *redundent* unless we can make detailed comparisons between EXP and DNS with satisfactory results, only then do we have the basic precondition to achieve the physical insight we seek.

From existing literature it is clear that the FST induced boundary-layer transition scenario in its very simplest case, i.e. for a zero-pressure gradient flow, we are still raising questions on the receptivity process and we do not seem to have reached a consensus on the break-down process of streamwise streaks into turbulent spots. It is therefore wise to take a closer look at existing DNS databases and to carry out detailed EXP matching these conditions, or alternatively, to carry out additional detailed EXP that can be computed with DNS. The two approaches, EXP and DNS, have both their pros and cons but where one's advantage is often the other's disadvantage (cf. Figure 1). One advantage of EXP is that it allows for parameter variation studies, like systematically varying the FST scales and turbulence intensity, which is not realistic to do with DNS. The amount of detailed information about the transition process is on the other hand superior with DNS compared to EXP, and the amount of data is often enormous which is why DNS data should always be made available through open access databases so that they can benefit everyone and, hence, be fully utilised.

The present contribution will focus on the current status, i.e. *what we do know* and *what we do not know* with certainty about this complex transition scenario. Recent progress on the importance of both the FST scales on the transition location and the sensitivity of the leading-edge pressure gradient to the receptivity process will be discussed based on EXP, and a direct comparison between EXP [1] and DNS [2] will be presented. To summarize, the following questions will be addressed, *are we satisfied with the outcome of this direct DNS-EXP comparison*? and, *how do we go about solving the FST induced transition puzzle*?

References

[1] S. B. Mamidala, A. Weingärtner, and J. H. M. Fransson. *Direct EXP-DNS comparision: EXP Campaign #3.* To be submitted, 2022.
[2] Data obtained from the Johns Hopkins Turbulence Databases (JHTDB) at: *http://turbulence.pha.jhu.edu*
[3] S. B. Mamidala, A. Weingärtner, and J. H. M. Fransson. *EXP Campaign #2.* To be submitted, 2022.

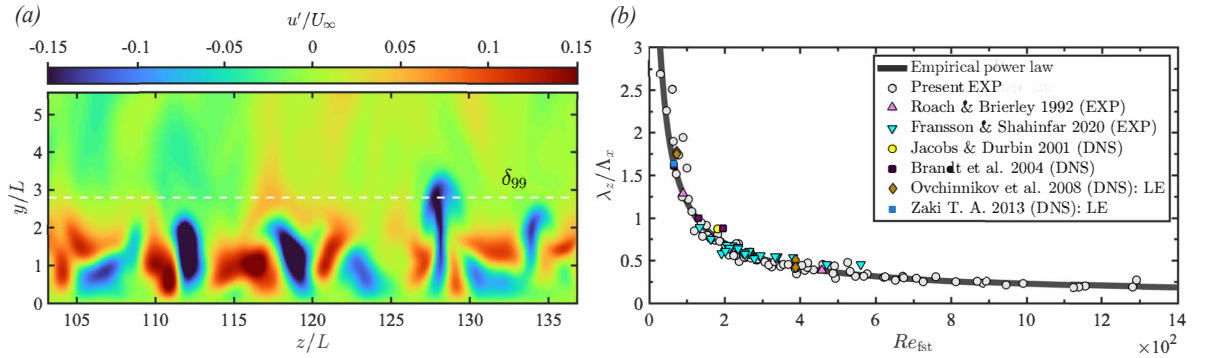

FIGURE 1. *(a) Cross-sectional snapshot of the disturbance structures inside the boundary layer at* $Re_x = 1.56 \times 10^5$ $(< Re_{tr} = 2.48 \times 10^5)$. *An example of detailed information using DNS [2]. (b) Correlation between* (λ_z/Λ_x) *and* $Re_{\text{fst}} = (\Lambda_x u_{\text{rms}}/\nu)_{x=0}$, *which is based on the FST integral length scale* (Λ_x), *the FST velocity standard deviation* (u_{rms}), *and the kinematic viscosity of the fluid* (ν). λ_z *denotes the spanwise averaged wavelength of the unsteady boundary-layer streaks at the onset of transition. An example of parameter variation study using EXP [3].*

EFFECTS OF FREE-STREAM TURBULENCE SCALE ON DISTURBANCE GROWTH ON AN AIRFOIL AND ITS RELATION TO OPTIMAL DISTURBANCES

José M. Faúndez Alarcón[1], Pierluigi Morra[1], Ardeshir Hanifi[1], Dan S. Henningson[1]
[1]*KTH Royal Institute of Technology, Linné FLOW Centre, SE-10044, Stockholm, Sweden*

Studying the response of the boundary-layer to external vortical disturbances, such as the case of free-stream turbulence, is a challenging problem due to the several steps involved in the receptivity process and the different flow configurations where this phenomena can take place. One of the most successful tools for this endeavour is optimal disturbance theory [1], which is able to describe many of the features observed in experiments. However, a common criticism is that optimal disturbances, as such, have never been measured in a real flow situation.

In the present work, we perform the stability analysis of the flow around a NACA0008 airfoil subjected to free-stream turbulence (FST). Direct Numerical Simulations (DNS), considering the leading edge, are carried out for a turbulence intensity (Tu) of 0.5% and two different spectra, which are characterised by their integral length scales L. Similarly to numerical [2] and experimental [3] results on flat plates, these simulations show the dependence of the streaks growth rate on the FST scales, as can be seen in figure 1a. By studying the optimal disturbances for our geometry, for instance with the results in figure 1b, we can expect faster decay for smaller disturbances scales, as the case $L = 0.0021$ in figure 1b. Moreover, we perform an explicit comparison between optimal disturbance theory and the simulations by projecting the DNS Fourier modes, at the leading edge, onto the optimal disturbances. This procedure allows us to properly scale the optimal growth and compare their evolution downstream with the Fourier modes. Some of these comparisons can be seen in figures 1c and 1d for specific Fourier modes corresponding to the cases $L = 0.01$ and $L = 0.0021$, respectively.

With these results, we show how the arbitrary and randomly generated Fourier modes not only evolve to the optimal shape, but also their growth is dictated by their optimal projection. Perhaps more important, for the first time we can place optimal disturbance theory in a more realistic flow situation, confirming its relevance to the study of free-stream turbulence induced disturbances.

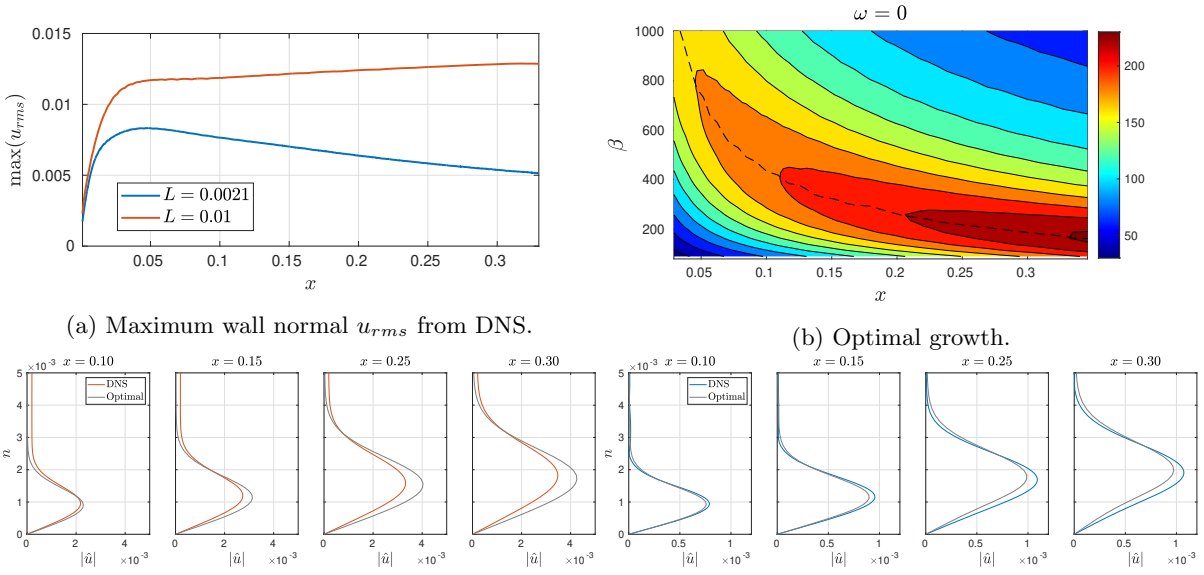

(a) Maximum wall normal u_{rms} from DNS.

(b) Optimal growth.

(c) Fourier mode for case $L = 0.01$.

(d) Fourier mode for case $L = 0.0021$.

Figure 1: Comparison between DNS results and optimal disturbance theory.

References

[1] P. Andersson, M. Berggren, and D. S. Henningson, "Optimal disturbances and bypass transition in boundary layers," *Physics of Fluids*, vol. 11, no. 1, pp. 134–150, 1999.

[2] L. Brandt, P. Schlatter, and D. S. Henningson, "Transition in boundary layers subject to free-stream turbulence," *Journal of Fluid Mechanics*, vol. 517, pp. 167–198, 2004.

[3] K. J. Westin, A. A. Bakchinov, V. V. Kozlov, and P. H. Alfredsson, "Experiments on localized disturbances in a flat plate boundary layer. Part 1. The receptivity and evolution of a localized free stream disturbance," *European Journal of Mechanics, B/Fluids*, vol. 17, no. 6, pp. 823–846, 1998.

INPUT-OUTPUT ANALYSIS OF BOUNDARY-LAYER TRANSITION DUE TO FREE-STREAM TURBULENCE

Diego C. P. Blanco[1], Kenzo Sasaki[2], Ardeshir Hanifi[2], Dan S. Henningson[2], André V. G. Cavalieri[1]

[1] *Divisão de Engenharia Aeroespacial, Instituto Tecnológico de Aeronáutica, 12228-900, São José dos Campos/SP - Brazil*

[2] *FLOW Turbulence Lab., Department of Engineering Mechanics, KTH Royal Institute of Technology, SE-10044 Stockholm, Sweden*

In the context of resolvent analysis the flow response to non-linear excitations can be quantified by linearising the Navier-Stokes (NS) equations, around either a laminar base solution [1] or a mean flow [2], and isolating non-linear terms as an input to the linear system. The output $\hat{\mathbf{y}}(\omega)$ and the non-linear forcing $\mathbf{B}_n\hat{\mathbf{f}}_n(\omega)$ are related by the resolvent operator $\mathbf{R}(\omega)$ via the state $\hat{\mathbf{q}}(\omega)$. In a general scenario of transition in a complex disturbance environment, such as a boundary layer subject to free-stream turbulence, two inputs to the system may be defined: upstream fluctuations $\hat{\mathbf{q}}_b$ and non-linear excitation $\hat{\mathbf{f}}_n$. An input-output framework may be defined as

$$\left\{\begin{array}{c} -\left(i\omega\mathbf{I}+\mathbf{L}\right)\hat{\mathbf{q}}=\hat{\mathbf{f}} \\ \hat{\mathbf{y}}=\mathbf{H}\hat{\mathbf{q}} \end{array}\right. \implies \hat{\mathbf{y}}=-\mathbf{H}\left(i\omega\mathbf{I}+\mathbf{L}\right)^{-1}\hat{\mathbf{f}} \therefore \left\{\begin{array}{c} \mathbf{R}=-\mathbf{H}\left(i\omega\mathbf{I}+\mathbf{L}\right)^{-1} \\ \hat{\mathbf{f}}=\mathbf{B}_n\hat{\mathbf{f}}_n+\mathbf{B}_b\hat{\mathbf{q}}_b \end{array}\right. \tag{1}$$

We separate the response in two distinct components: the linear response to external excitations $\hat{\mathbf{y}}_b = \mathbf{R}\mathbf{B}_b\hat{\mathbf{q}}_b$ and the response to non-linear forcing $\hat{\mathbf{y}}_f = \mathbf{R}\mathbf{B}_n\hat{\mathbf{f}}_n$. Thus, we have the equation for the response's cross spectral density (CSD) tensor $CSD_{\hat{\mathbf{y}}\hat{\mathbf{y}}} = \mathcal{E}\left(\hat{\mathbf{y}}\hat{\mathbf{y}}^H\right) = \mathbf{R}\mathbf{B}_b\mathcal{E}\left(\hat{\mathbf{q}}_b\hat{\mathbf{q}}_b^H\right)\mathbf{B}_b^H\mathbf{R}^H + \mathbf{R}\mathbf{B}_n\mathcal{E}\left(\hat{\mathbf{f}}_n\hat{\mathbf{f}}_n^H\right)\mathbf{B}_n^H\mathbf{R}^H$, meaning that the statistics can be reconstructed from the inputs. This is a useful feature in the study of transition to turbulence as it allows the identification of linear and non-linear mechanisms of receptivity in instances when the forcing component is of complex nature.

We demonstrate this procedure by analysing a large-eddy simulation (LES) of a boundary layer over a flat plate without leading edge ($Re^* = 300$ at the intake), subject to 3% free stream turbulence level. The domain is periodic in the span and flow directions, with a fringe zone at the downstream region. The non-linear terms of the NS equations $\hat{\mathbf{f}}_n = [\hat{\mathbf{f}}_x, \hat{\mathbf{f}}_y, \hat{\mathbf{f}}_z]^T$ are computed from the snapshots of the velocity field $\mathbf{y} = [\hat{\mathbf{u}}, \hat{\mathbf{v}}, \hat{\mathbf{w}}]^T$ at each time step. The state is defined as $\mathbf{q} = [\hat{\mathbf{u}}, \hat{\mathbf{v}}, \hat{\mathbf{w}}, \hat{\mathbf{p}}]^T$ and spectral estimation is done via the Welch method [3]. In this case, the term $\mathbf{B}_b\hat{\mathbf{q}}_b$ is the fringe forcing capable of generating the intake conditions observed in the LES. Figure 1 shows the results of the PSD (diagonal of the CSD tensor) reconstruction for the most energetic pair frequency/spanwise wavenumber, in which we find that streaks in the boundary layer are mainly the result of a non-linear receptivity mechanism, for this case.

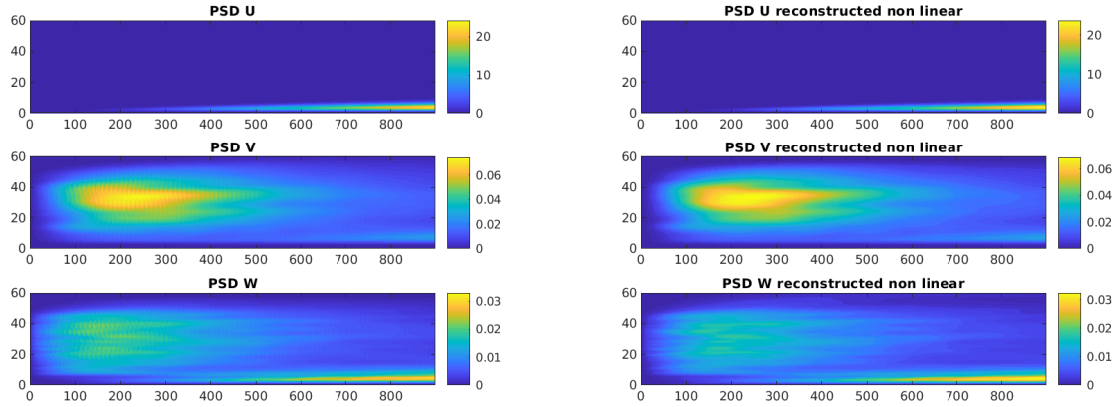

FIGURE 1. *Left, PSD for* $(\omega, \beta) = (0.0098, 0.3770)$. *Right, PSD reconstruction using only the non-linear forcing.*

References

[1] Mihailo R. Jovanović and Bassam Bamieh. Componentwise energy amplification in channel flows. *Journal of Fluid Mechanics*, 534:145–183, 2005.

[2] Beverly J. McKeon and Ati S. Sharma. A critical-layer framework for turbulent pipe flow. *Journal of Fluid Mechanics*, 658:336–382, 2010.

[3] Peter D. Welch. The use of fast fourier transform for the estimation of power spectra: A method based on time averaging over short, modified periodograms. *IEEE Transactions on Audio and Electroacoustics*, 15(2):70–73, 1967.

LINEAR STABILITY ANALYSIS ON A LAMINAR SEPARATION BUBBLE SUBJECTED TO FREESTREAM TURBULENCE

Thomas Jaroslawski[1], Maxime Forte[1], Olivier Vermeersch[1], Erwin Gowree[2], Jean-Marc Moschetta[2]
[1] *ONERA, Toulouse, France*
[2] *ISAE-SUPAERO, Toulouse, France.*

Boundary layer measurements using hotwire anemometry are employed to study the flow development of a laminar separation bubble (LSB) over the suction side of a NACA0015 aerofoil, at a chord based Reynolds number of 125000 fixed and at an angle of incidence of 2.3 degrees, in a open circuit wind tunnel subjected to a wide range of turbulence intensity ($0.15\% < Tu < 6.26\%$). A Local linear stability analysis (LST) is conducted on experimental boundary layer profiles in the fore position of the LSB (cf. Fig. 1). LST is shown to accurately model incipient disturbance growth, unstable frequencies and eigenfunctions for configurations subjected to levels of Tu up to 3%, suggesting modal growth of instabilities, even at elevated levels of Tu. Additionally, the presence of streaks is highly probable for configurations with $Tu > 1\%$, with unfiltered wall-normal disturbance profiles agreeing remarkably well with the optimal perturbation profile proposed by Luchini et al. (2000), cf. Fig, 2. This observation leads to the conclusion that the co-existence of both modal and non-modal convective growth of instabilities is present in the LSB, providing experimental confirmation of the numerical simulations by Hosseinverdi and Fasel (2019). Furthermore, increasing the Tu resulted in the range of unstable frequencies to decrease and the Reynolds number dependence to increase due the inflection point shifting closer towards the wall. This suggests that a viscous, rather than an invicid formulation of the stability equations is appropriate for modeling modal instabilities in the fore portion of the current LSB, especially in the presence of freestream turbulence. It is ascertained that streaks (non-modal instability) modify the mean flow field, resulting in an increased importance of viscosity, which contributes to the the damping of the convective growth of modal instabilities in the LSB.

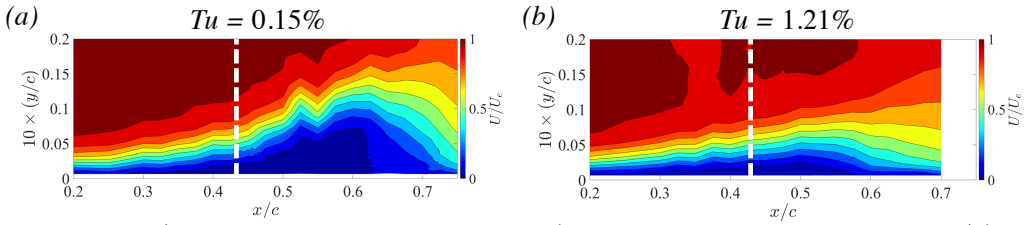

FIGURE 1. *Contours (21 chordwise boundary layer profiles) of the mean streamwise velocity for (a) the natural case and (b) the case with freestream turbulence forcing. White line denotes the location of local LST analysis.*

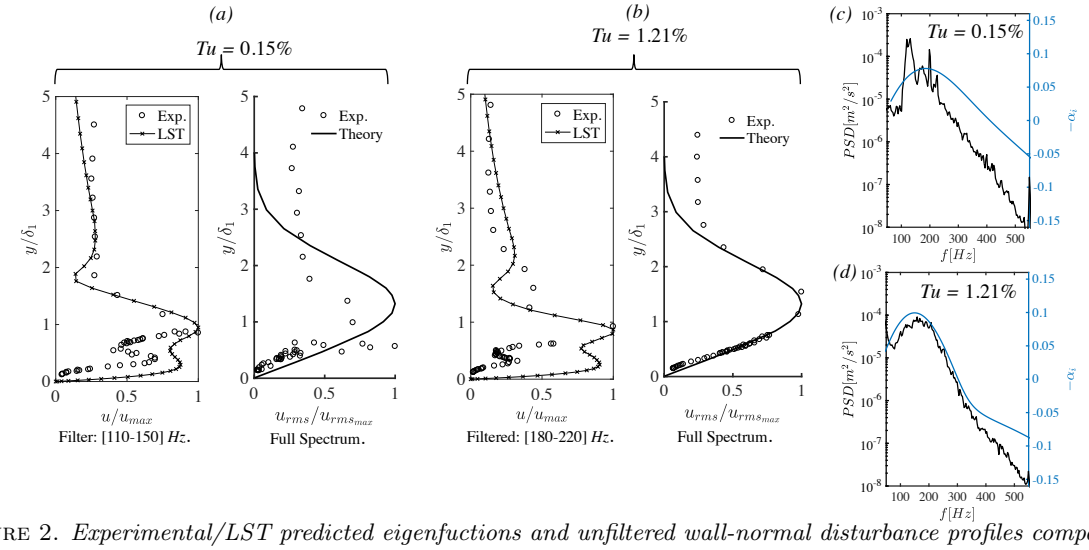

FIGURE 2. *Experimental/LST predicted eigenfuctions and unfiltered wall-normal disturbance profiles compared to theoretical predictions by Luchini et. al (2000) for (a) the natural case and (b) the case with freestream turbulence forcing. Comparison between the amplified frequencies predicted by LST and measured in the experiment (c,d)*

References

[1] Luchini, P. Reynolds-number-independent instability of the boundary layer over a flat surface: optimal perturbations. *Journal of Fluid Mechanics*, 404, 289–309, 2000.
[2] Hosseinverdi, S., Fasel, H. F. Numerical investigation of laminar–turbulent transition in laminar separation bubbles: the effect of free-stream turbulence. *Journal of Fluid Mechanics*, 867858, 714–759, 2019.

MODAL STABILITY ANALYSIS OF TOROIDAL PIPE FLOW APPROACHING ZERO CURVATURE

Valerio Lupi[1], Jacopo Canton[2], Enrico Rinaldi[1], Ramis Örlü[1], Philipp Schlatter[1]
[1] *FLOW/SimEx, KTH Royal Institute of Technology, SE-100 44 Stockholm, Sweden*
[2] *Institute for Atmospheric and Climate Science, ETH Zurich, CH-8092 Zurich, Switzerland*

The flow in a straight pipe was found to be linearly stable up to $Re_b = 10^7$ by Meseguer & Trefethen [1], with Re_b being the Reynolds number based on bulk velocity, diameter and kinematic viscosity. The authors also derived an asymptotic expression of the growth rate to show that the linear stability threshold for the straight pipe flow is infinite. However, contrary to plane Couette flow [2], there is no analytical proof for this result in the literature. Indeed, the expression provided by [1] is an extrapolation based on their numerical data. The purpose of the present work is to study the linear stability of the flow in a torus for very low curvatures approaching zero, i.e. the straight pipe, and to provide further evidence of the result in [1]. We perform classical linear stability analysis. Both the base flow computation and the modal stability analysis are carried out using an in-house developed code, which employs a spectral collocation method based on Chebychev nodes in the radial direction and Fourier nodes in the azimuthal one. Proper treatment of the pressure boundary conditions is performed to avoid spurious pressure modes in the base flow computation. The analysis is similar to the BiGlobal stability approach, with the difference of employing a three-dimensional base flow instead of a two-dimensional one. A sensitivity analysis of the stability properties with respect to the underlying base flow is carried out by linearizing around both the computed base flow and the Hagen–Poiseuille velocity profile. In the latter case, the perturbations are allowed to have non-zero curvature. The results show that a proper account of the secondary motion in the base flow is needed to correctly capture the spectrum of the linearized Navier–Stokes operator. The analysis cannot be repeated using the Dean's approximation [4] as base flow, since this solution ceases to be valid for values of curvature and Reynolds number at criticality. Curvatures below 10^{-2} are investigated, and a continuation method is employed to track the most unstable eigenmodes. The tracking is performed by Rayleigh quotient iteration. A wide range of streamwise wavenumbers needs to be taken into account, in order not to miss unstable branches. The neutral curve obtained with preliminary results is shown in the figure below. It indicates that the critical Reynolds number increases with curvature, suggesting that it might go asymptotically to infinity as $\delta \to 0$, i.e. approaching the straight pipe.

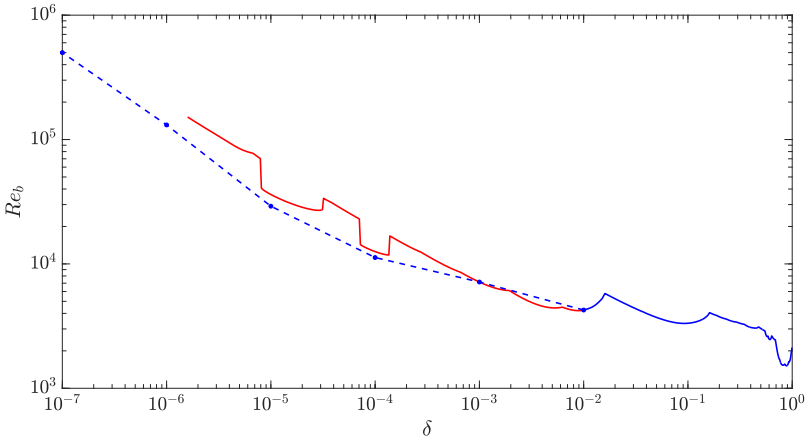

FIGURE 1. *Neutral curve in the $\delta - Re_b$ plane for curvatures $\delta \in [10^{-7}, 1]$. The blue solid line is taken from [5], the red solid line represents data from the present study, the blue dashed line is an exploratory curve obtained performing full spectrum computation at different curvatures.*

References

[1] Á. Meseguer, L. N. Trefethen. Linearized pipe flow to Reynolds number 10^7. *J. Comput. Phys.*, 186(1):178–197, 2003.
[2] V. A. Romanov. Stability of plane-parallel Couette flow. *Funct. Anal. Appl.*, 7(2):137–146, 1973.
[3] J. Canton. *Of Pipes and Bends.* , PhD thesis, KTH Royal Institute of Technology, 2018.
[4] W. R. Dean. Note on the motion of fluid in a curved pipe. *Lond. Edinb. Dubl. Philos. Mag. J. Sci.*, 4(20):208–223, 1927.
[5] J. Canton, P. Schlatter, R. Örlü. Modal instability of the flow in a toroidal pipe. *J. Fluid Mech.*, 792:894–909, 2016

TRANSIENT GROWTH IN ASYMPTOTIC PULSATING CHANNEL FLOW

J. S. Kern, A. Hanifi, D. S. Henningson
FLOW, Department of Engineering Mechanics, KTH Royal Institute of Technology, Stockholm, Sweden

Transient growth, the short-time amplification of linear perturbations due to the interaction of non-orthogonal eigendirections, is a fundamental phenomenon for non-normal operators that has been extensively studied for steady flows. For these configurations, transient growth is synonymous with *initial* transient growth studied in the context of optimal disturbances since the asymptotic fate of linear perturbations is dictated by the operator's spectrum. In time-dependent flows in general, and in particular in periodic configurations, this is not the case. In this case, the linear operator changes in time and even in the time-asymptotic state, i.e. the periodic orbit, the necessary conditions for instantaneous transient growth can be present.

In this study, we study the behaviour of linear perturbations about the the time-periodic channel flow superimposed with a pulsatile component driven by a sinusoidal pressure gradient for which an analytical expression for the the base flow exists. The relevant parameters are the Reynolds number (Re) of the steady base flow, the frequency parameter (Womersley number, Wo) of the pulsations and their amplitude ($\tilde{Q}$) defined as

$$\mathrm{Re} = \frac{U_c h}{\nu}, \qquad \mathrm{Wo} = h\sqrt{\frac{\Omega}{\nu}}, \qquad \tilde{Q} = \frac{Q_1}{Q_0}, \tag{1}$$

where U_c is the centerline velocity of the steady component, h is the channel half-height, ν is the kinematic viscosity, Ω is the pulsation frequency and Q_i the the mass flow rates of the steady (subscript 0) and unsteady (subscript 1) components, respectively. As the pulsation amplitude is increased, the periodic orbit exhibits growth rate modulations and abrupt transitions from decay to amplification as shown in Fig. 1 that have also emerged, although not always specifically highlighted, in other studies ([3, 4, 1]).

We describe the emergence of subharmonic eigenvalue orbits in the instantaneous operator due to spectral degeneracies (see the leading eigenvalue in Fig. 1, [2]) and relate the abrupt growth rate variations with eigenvalue branch transitions which take place via non-normal transient growth bursts in the asymptotic solution that follow a similar path as the Orr mechanism relevant for optimal initial transient growth of purely two-dimensional disturbances.

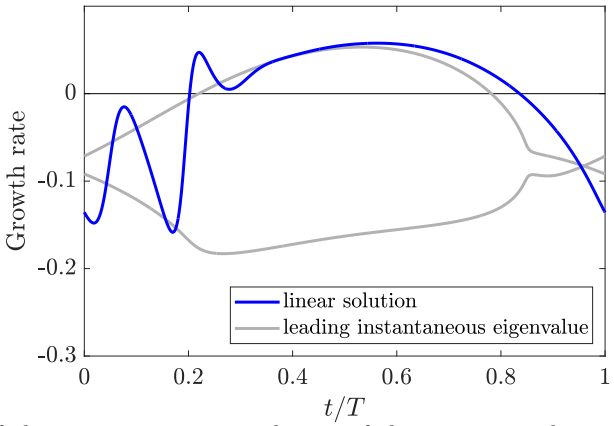

FIGURE 1. *Comparison of the instantaneous growth rate of the asymptotic linear solution over one pulsation period (T) with the leading instantaneous eigenvalue which is subharmonic with period $2T$. Parameter values: $Re = 7500$, $Wo = 18, \tilde{Q} = 0.16$.*

References

[1] J.S. Kern, M. Beneitez, A. Hanifi, and D.S. Henningson. Transient linear stability of pulsating Poiseuille flow using optimally time-dependent modes. *J. Fluid Mech.*, 927:A6, 2021.
[2] J.S. Kern, A. Hanifi, and D.S. Henningson. Subharmonic eigenvalue orbits in pulsating Poiseuille flow. *To be published in J. Fluid Mech.*
[3] B. Pier and P. J. Schmid. Linear and nonlinear dynamics of pulsatile channel flow. *J. Fluid Mech.*, 815:435–480, 2017.
[4] B. Pier and P. J. Schmid. Optimal energy growth in pulsatile channel and pipe flows. *J. Fluid Mech.*, 926:A11, 2021.

FINITE-TIME STABILITY OF AN OPTIMAL EDGE TRAJECTORY IN THE BLASIUS BOUNDARY LAYER

M. Beneitez[1], Y. Duguet[2], P. Schlatter[3] and D. S. Henningson[3]
[1]*DAMTP, Centre for Mathematical Sciences, Wilberforce Road, Cambridge CB3 0WA, UK*
[2]*LISN-CNRS, Campus Universitaire d'Orsay, Université Paris-Saclay, F-91400, Orsay, France*
[3]*FLOW Centre and SeRC, KTH Engineering Mechanics, Royal Institute of Technology, SE-100 44 Stockholm, Sweden*

Bypass transition to turbulence in three-dimensional boundary layer flows is characterised by the breakdown of streamwise streaks. In the context of computational linear stability analysis, the choice of a physically appropriate base flow compatible with streak breakdown is not obvious. In this talk, rather than the laminar base flow, the linear stability analysis of an unsteady transient initialised by the minimal seed, which is optimal in terms of initial kinetic energy, is considered. The associated base flow is unsteady, free from any spatial symmetry, and belongs to the laminar-turbulent separatrix for a finite time only.

A finite-time generalisation of modal linear stability analysis, allowing for arbitrarily unsteady base flows, is therefore required. The recently developed optimally time-dependent (OTD) modes [1] are chosen as a finite-dimensional projection basis for the finite-time stability analysis. OTD modes, computed on the fly, approximate optimally the linearised dynamics under the constraint of forming an orthonormal basis. We assess the ability of the leading OTD modes to describe transient instabilities of an optimal edge trajectory [2], initiated with the recently computed minimal seed [3]. The leading subspace spanned by 8 OTD modes appears always unstable, owing to both modal and non-modal growth mechanisms. The OTD modes identify well the physical spatial regions along the edge trajectory showing the largest instantaneous growth.

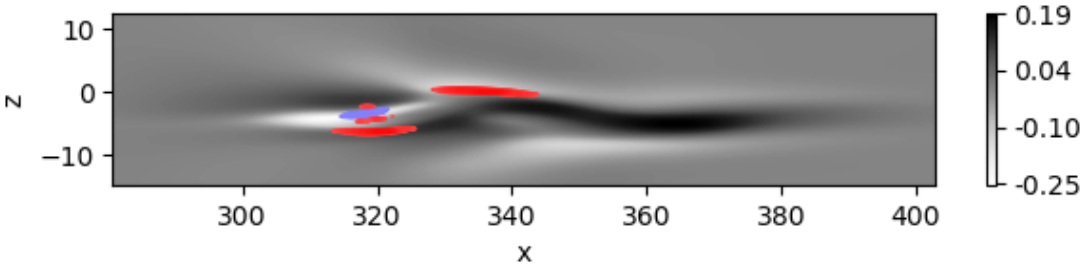

FIGURE 1. *Two-dimensional greyscale planes of the perturbation velocity of the edge trajectory overlapped with contour lines of the ω_y, for the leading projected OTD mode $\{u_1^\lambda\}$ corresponding to 40% to 100% of its maximum value. Plane xz for $y = 2.5$, flow from left to right.*

References

[1] H. Babaee, and T. P. Sapsis. minimization principle for the description of modesassociated with finite-time instabilities. *Proc. R. Soc. Lond. A*, **472**, 20150779, 2016.
[2] M. Beneitez, Y. Duguet, P. Schlatter and D. S. Henningson. Edge tracking in spatially developing boundary layer flows. *J. Fluid Mech.*, **881**, 164-181, 2019.
[3] C. Vavaliaris, M. Beneitez, and D. S. Henningson. Optimal perturbations and transition energy thresholds in boundary layer shear flows. *Phys. Rev. Fluids*, **5**, 062401(R), 2020.

REVISITING THE O(2) EQUIVARIANT STEADY–HOPF INTERACTION

Javier Sierra-Ausin[1,2], David Fabre[2], and Edgar Knobloch[3]
[1] *Dipartimento di Ingegneria Industriale (DIIN), UNISA, Fisciano 84084, Italy*
[2] *Institut de Mécanique des Fluides de Toulouse (IMFT), Toulouse 31400, France.*
[3] *Department of Physics, University of California at Berkeley, Berkeley, California 94720, USA*

We consider the mode-interaction between a steady-state bifurcation and Hopf bifurcation in a system with $O(2)$ symmetry. It is somehow a natural configuration that emerges in many fluids of interest: Taylor–Couette flow (TCF), the wake flow of axisymmetric objects (WFA) and the wake of axisymmetric objects in mixed convection (WFA-MC). In here we analyse the bifurcation scenario of the WFA-MC problem for two axisymmetric bodies, a disk with variable thickness and the sphere. In this cases the flow state $\mathbf{q} = [\mathbf{u}, p]$ composed of the velocity field and the hydrodynamic pressure (the WFA-MC also includes the temperature field T) is decomposed as:

$$\mathbf{q} = \mathbf{Q}_0 + \mathrm{Re}\big[a_0(t)e^{-i\theta}\hat{\mathbf{u}}_s\big] + \ \mathrm{Re}\big[a_1(t)e^{-i\theta}\hat{\mathbf{u}}_{h,-1} + a_2(t)e^{i\theta}\hat{\mathbf{u}}_{h,1}\big] \tag{1}$$

Here $\mathbf{Q}_0$ is the steady-state flow state that is invariant under the action of the whole $O(2)$ group, $\hat{\mathbf{u}}_s$ is the steady mode and $\hat{\mathbf{u}}_h$ is the Hopf (unsteady) mode. The ansatz eq. (1) takes into account the continuous symmetry by the term $e^{\pm i\theta}$, where $\theta \in S^1$ is an angle-like variable in the periodicity direction.
Using the polar representation of the complex amplitudes $a_j = r_j e^{i\phi_j}$ for $j = 0, 1, 2$, the normal form is recast to a system of four coupled equations governing the amplitudes r_0, r_1, r_2 and the mixed phase $\Psi = \phi_1 - \phi_2 - 2\phi_0$:

$$\begin{aligned}
\dot{r}_0 &= \big[\lambda_s + l_0 r_0^2 + l_1\big(r_1^2 + r_2^2\big)\big] r_0 + l_3 r_0 r_1 r_2 \cos\Psi \\
\dot{r}_1 &= \big[\lambda_h + B_r r_1^2 + (A_r + B_r) r_2^2 + C_r r_0^2\big] r_1 + r_0^2 r_2\big(D_r \cos\Psi + D_i \sin\Psi\big) \\
\dot{r}_2 &= \big[\lambda_h + B_r r_2^2 + (A_r + B_r) r_1^2 + C_r r_0^2\big] r_2 + r_0^2 r_1\big(D_r \cos\Psi - D_i \sin\Psi\big) \\
\dot{\Psi} &= (A_i - 2l_2)(r_2^2 - r_1^2) - 2l_3 r_1 r_2 \sin\Psi + r_0^2 D_i \cos\Psi \left[\tfrac{r_2}{r_1} - \tfrac{r_1}{r_2}\right] - r_0^2 D_r \sin\Psi \left[\tfrac{r_2}{r_1} + \tfrac{r_1}{r_2}\right]
\end{aligned} \tag{2}$$

The unfolding of the normal form allows a characterization of the nonlinear states observed in the transition to complex dynamics in these flow configurations. Fig 1 displays the distinct spatio-temporal structures of the flow field in the WFA-MC (thick disk, opposing flow) problem.

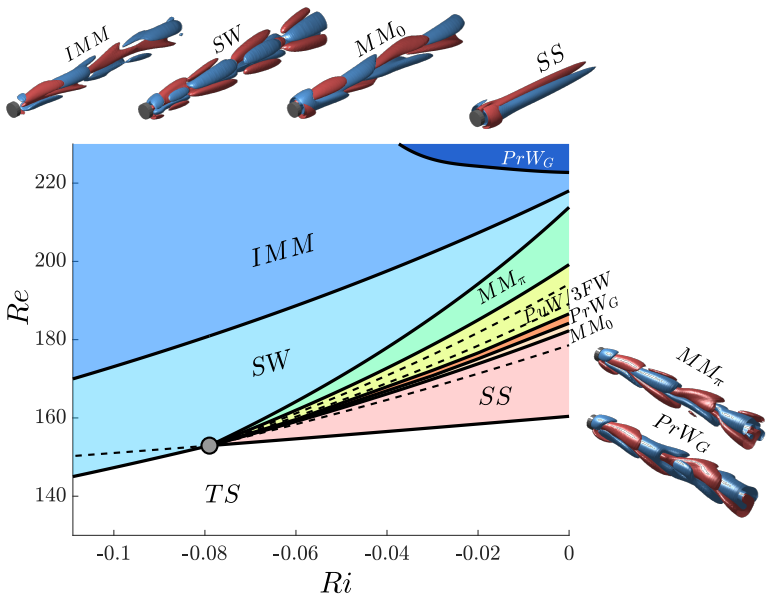

Figure 1: Parametric map of the patterns within the flow past a thick disk (aspect ratio $\chi = 3$) in mixed convection (opposing flow) conditions. Re denotes the Reynolds number and Ri the Richardson number.

WEAKLY NONLINEAR EVOLUTION OF STOCHASTICALLY DRIVEN NON-NORMAL SYSTEMS.

Yves-Marie Ducimetière[1], Edouard Boujo[1], François Gallaire[1]
[1] *Laboratory of Fluid Mechanics and Instabilities, EPFL, CH1015 Lausanne, Switzerland*

We consider nonlinear dynamical systems driven by a stochastic forcing. It has been largely evidenced in the literature that the linear response of nonnormal systems may exhibit a large variance amplification even in a linearly stable regime. It is typically the case for some parallel or nonparallel fluid flows, governed by the Navier-Stokes equations [1, 2, 3].

However, the linear response is relevant only in the limit of vanishing forcing intensity. As the latter increases, the spectrum and the variance of the response may be strongly modified, owing to nonlinear effects [4].

To go beyond this limitation, we propose a theoretical approach to derive an amplitude equations governing the weakly nonlinear evolution of these systems. This approach, contrarily to classical ones, does not rely on the presence of an eigenvalue close to the neutral axis, and the Fourier components of the response are allowed to be arbitrarily different from any eigenmode. It applies to any sufficiently nonnormal operator, and reconciles the nonnormal nature of the growth mechanisms with the need for a centre manifold to project the leading-order dynamics.

The methodology is outlined for a generic nonlinear dynamical system, and the application case highlights a common [3] nonnormal mechanism in hydrodynamics: the convective nonnormal amplification in the flow past a backward-facing step. At low numerical cost, the amplitude equation quantifies the respective contribution of each dominant nonlinear interaction, thus bringing insight on the saturation mechanisms of the stochastic amplification.

References

[1] B. Farrell, and P. Ioannou. Stochastic forcing of the linearized Navier–Stokes equations. *Phys. Fluids A*, 5(11):2600–2609, 1993.
[2] J. Fontane, P. Brancher, and D. Fabre. Stochastic forcing of the Lamb–Oseen vortex. *J. Fluid Mech.*, 613:233–254, 2008.
[3] G. Dergham, D. Sipp, and J. Robinet. Stochastic dynamics and model reduction of amplifier flows: The backward facing step flow. *J. Fluid Mech.*, 719:406–430, 2013.
[4] V. Mantic-Lugo, and F. Gallaire. Saturation of the response to stochastic forcing in two-dimensional backward-facing step flow: A self-consistent approximation. *Phys. Rev. Fluids* , 1(8):083602, 2016.

REDUCED ORDER MODELS COMBINING MODAL DECOMPOSITIONS AND MACHINE LEARNING TOOLS

Soledad Le Clainche[1]
[1] *School of Aerospace Engineering, Universidad Politécnica de Madrid, E-28040, Spain*

Halting climate change is one of the greatest challenges facing our society. To mitigate its effects, it is necessary to look for alternatives and develop new technologies that are capable of reducing atmospheric pollution. Fluid mechanics is a science with multiple applications that can be used for this purpose, some examples include: improving efficiency in combustion systems, studying ways to reduce air pollution in urban flows or improving aeronautical designs and making them more efficient. To study these problems we propose to develop reduced order models (ROMs) based on physical principles using (i) modal decompositions (i.e., singular value decomposition - SVD [1], higher order dynamic mode decomposition - HODMD [2]) and (ii) machine learning tools (neural networks) combined with the previous decompositions [3, 4]. In this work, these techniques will be applied to solve the aforementioned problems, and new strategies for developing efficient and accurate ROMs will be presented.

References

[1] Sirovich L. *Turbulence and the dynamics of coherent structures. Parts I - III*, Quart. Appl. Math., 45(3):561-571, 1987.
[2] Le Clainche S., Vega J.M. *Higher order dynamic mode decomposition*, SIAM J. Appl. Dyn. Sys., 16(2):882-925, 2017.
[3] Abadía-Heredia, R., López-Martín, M., Carro, B., Arribas, J.I., Pérez, J.M., Le Clainche, S., *A predictive hybrid reduced order model based on proper orthogonal decomposition combined with deep learning architectures*, Exp. Syst. Appl. , 2021.
[4] López-Martín, M., Le Clainche, S., Carro, B. *Model-free short-term fluid dynamics estimator with a deep 3D-convolutional neural network*, Exp. Syst. Appl., 177:114924, 2021.

DERIVATIVE-FREE OPTIMIZATION OF THE FLOW AROUND AN AIRFOIL USING A CUT CELL METHOD BASED SOLVER

Alejandro Quirós Rodríguez[1], Tomas Fullana[1], Vincent Le Chenadec[2], Miguel Fosas de Pando[3], Taraneh Sayadi[1]

[1] *Sorbonne Université, Institut Jean le Rond d'Alembert, IJLRA, F-75005 Paris, France*
alejandro.quiros_rodriguez@etu.sorbonne-universite.fr
tomas.fullana@sorbonne-universite.fr
taraneh.sayadi@sorbonne-universite.fr
[2] *MSME, Université Gustave Eiffel, UPEC, CNRS, F-77454 Marne-la-Vallée, France*
vincent.lechenadec@u-pem.fr
[3] *Universidad de Cádiz, Departamento de Ingeniería Mecánica y Diseño Industrial, 11519 Puerto Real, Spain*
miguel.fosas@uca.es,

Optimization algorithms can be classified in two categories, gradient-based and derivative-free methods. Gradient-based algorithms present a faster converge rate, but their performance drop when the objective function contains multiple local minima. As a result, their application to configurations that exhibit complex flow features does not provide optimal results. Derivative-free algorithms can overcome this difficulty by ensuring convergence to global minimum at the cost of increasing the number of function evaluations.

In this work, the derivative-free surrogate model based optimization algorithm DYnamic COordinate search using Response Surfaces (DYCORS) [1] is adopted to optimize the flow around a NACA airfoil at various Reynolds numbers. The drag coefficient is selected as the objective function and multiple actuation strategies, such as volume forcing and surface blowing are compared. The derivative-free algorithm is found to gradient-based algorithms when a large set of control parameters and a complex enough objective function is employed [2].

The simulations are performed using an energy-conservative cut cell method [3]. The incompressible Navier-Stokes equations are discretized by means of the Marker-And-Cell (MAC) method where vector field components are located at face centers and scalar fields at cell centers. Time-advancement is performed with an implicit-explicit Runge-Kutta scheme. The solid boundary is specified using the level set method, where the boundary is defined as the zero-contour of a scalar field. The discrete operators obtained with this cut cell method retain the structure of their continuous counterparts, i.e. the symmetry and skew-symmetry of the diffusive and convective transport operators, respectively and local and global energy conservation. The cut cell method provides an excellent tool to perform high-fidelity simulations of flows in complex geometries due to its reliance on Cartesian grids, which greatly reduces the complexity of the mesh generation process.

References

[1] R. G. Regis, and C. A. Shoemaker. Combining radial basis function surrogates and dynamic coordinate search in high-dimensional expensive black-box optimization. *Engineering Optimization*, 45(5):529–555, 2013.
[2] A. Quirós Rodríguez, M. Fosas de Pando, and T. Sayadi. Stochastic optimization of the flow around a linear cascade of blades. *in preparation.*
[3] T. Fullana, A. Quirós Rodríguez, V. Le Chenadec, and T. Sayadi. C^4: A Conservative Cartesian Cut Cell Method for the Solution of the Incompressible Navier-Stokes Equations for Staggered Meshes. *in preparation.*
[4] Y. Morinishi, T. S. Lund, O. V. Vasilyev, and P. Moin. Fully Conservative Higher Order Finite Difference Schemes for Incompressible Flow. *Journal of Computational Physics*, 143(1):90–124, 1998.

THE WIENER-HOPF METHOD APPLIED TO EXPERIMENTAL BOUNDARY LAYER CONTROL

Diego B. S. Audiffred[1], André V. G. Cavalieri[1], Pedro Paulo C. Brito[1], Eduardo Martini[2]
[1] *Instituto Tecnológico de Aeronáutica, São José dos Campos - Brazil*
[2] *Université de Poitiers, Poitiers - France*

Experimental control of Tollmien-Schlichting (TS) waves, based on the Wiener-Hopf control approach, was carried out in order to delay the transition to turbulence for the flow around an airfoil. The experiments were performed for a chord based Reynolds number of $5.33 \cdot 10^5$, using a NACA 0008 wing profile instrumented with pressure sensors and a plasma actuator. The schematic of the control system is shown in Figure 1a, where in $\mathbf{d}$ a disturbance is applied to trigger the TS waves; $\mathbf{z}$ is the control target and $\mathbf{u}$ is the actuation obtained with the kernel Γ, based on the sensor readings in $\mathbf{y}$, according to the expression: $\mathbf{u}(\omega) = \mathbf{\Gamma}(\omega)\mathbf{y}(\omega)$. Thus, in the time domain the actuation results from the convolution $\mathbf{u}(t) = \int_{-\infty}^{\infty} \mathbf{\Gamma}(\tau)\mathbf{y}(t-\tau)d\tau$.
When the kernel is obtained in the frequency domain, there is no guarantee it will be causal, that is, in the time domain it might be non-zero for negative values of τ, which means that the actuation signal depends on sensor readings that cannot be accessed in real-time applications. However, neglecting the non-causal part of the kernel, by simply truncating it to its causal part, may result in a significant drop in control performance [1, 2]. Optimal causal control might be achieved by using Lagrange multipliers in a quadratic functional cost that is minimized with respect to the kernel. This will lead to a Wiener-Hopf equation that can be solved with factorization of the equation terms into components that are regular on the upper and lower halves of the complex plane, referred to with + and − subscripts, respectively. This is shown by:

$$\mathbf{H}(\omega)\mathbf{\Gamma}_+(\omega)\hat{\mathbf{G}}(\omega) + \hat{\mathbf{\Lambda}}_-(\omega) = \hat{\mathbf{h}}(\omega)\mathbf{C_z}\hat{\mathbf{g}}(\omega) \xrightarrow{Factorization} \hat{\mathbf{\Gamma}}_+ = \hat{\mathbf{H}}_+^{-1}(\hat{\mathbf{H}}_-^{-1}\mathbf{C_z}\hat{\mathbf{h}}\hat{\mathbf{g}}\hat{\mathbf{G}}_-^{-1})_+\hat{\mathbf{G}}_+^{-1}. \quad (1)$$

$\mathbf{G}$ and $\mathbf{g}$ are functions related to the transfer function between $\mathbf{u}$ and $\mathbf{z}$; $\mathbf{\Lambda}_-$ is the Lagrange multiplier used to impose causality; $\mathbf{H}$ is the power spectral density (PSD) of the signals in $\mathbf{y}$; and $\mathbf{h}$ is the cross spectral density (CSD) between signals $\mathbf{y}$ and $\mathbf{z}$. Experimental results obtained with the Wiener-Hopf kernel were compared with the inverse feed-forward control (IFFC) method [3]. The Wiener-Hopf kernel could successfully attenuate the TS waves signals measured over the wing profile, yielding better results than the IFFC method as shown in Figure 1b. This demonstrates the applicability of the Wiener-Hopf method for flow control applications, with kernels obtained directly from statistics of inputs and outputs, avoiding the need of reduced-order models.

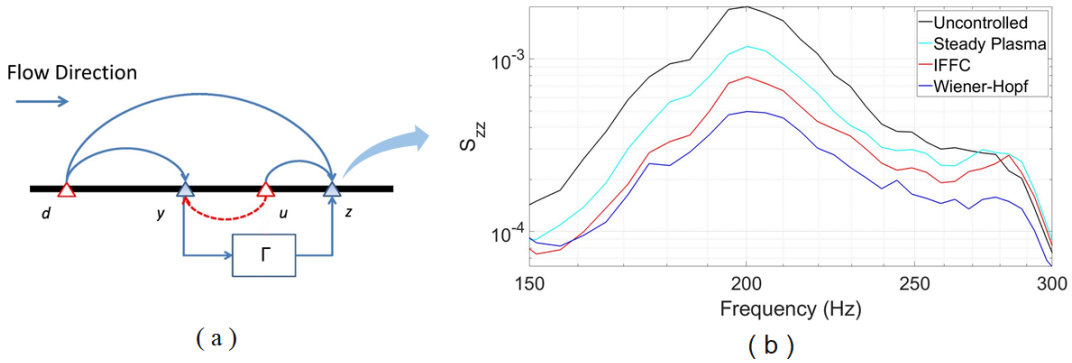

FIGURE 1. *(a) Schematic of the feed-forward control applied to the attenuation of TS waves. Adapted from [3]. (b) PSD of the uncontrolled and controlled signals in z.*

References

[1] Pedro P. C. Brito and Pierluigi Morra and André V. G. Cavalieri and Tiago B. Araújo and Dan S. Henningson and Ardeshir Hanifi *Experimental control of Tollmien–Schlichting waves using pressure sensors and plasma actuators.* Springer Science and Business Media LLC. *Experiments in Fluids*, 62(2), January 2021.
[2] Eduardo Martini and Junoh Jung and André V. G. Cavalieri and Peter Jordan and Aaron Towne. *Resolvent-based tools for optimal estimation and control via the Wiener-Hopf formalism. Phys. Fluid Dynamics*, 2022.
[3] Kenzo Sasaki and Pierluigi Morra and Nicoló Fabbiane and André V. G. Cavalieri and Ardeshir Hanifi and Dan S. Henningson *On the wave-cancelling nature of boundary layer flow control.* Springer Science and Business Media LLC. *Theoretical and Computational Fluid Dynamics*, 32(5):593–616, 2018.

NEAR WALL TURBULENCE CONTROL USING CIRCULAR CAVITIES

Francesco Scarano[1], Erwin R. Gowree[1], Marc C. Jacob[2]

[1] *Dep. of Aerodynamics and Propulsion ISAE - SUPAERO*

[2] *Lab. de Mécanique des Fluides et d'Acoustique, UMR 5509 CNRS, Université de Lyon, Ecole Centrale de Lyon, INSA Lyon, Université Claude Bernard Lyon I*

Drag reduction is nowadays a major task in civil aviation. The Advisory Council of Aeronautics Research in Europe (ACARE) has recently prescribed 75% cut of CO_2 emissions per passenger-mile with respect to 2000's level. In cruise condition, 1% of drag reduction is translated into a 0.75% in fuel-burn savings [4]. The turbulent boundary layer developing of an aircraft surfaces is responsible for almost 60% of the total drag in cruise condition.

The passive control of near wall turbulence by means of a staggered array of cavity is addressed in the paper. Accurate boundary layer surveys and Particle Image Velocimetry (PIV) measurements are conducted in the low speed wind tunnel of ISAE-SUPAERO. The test model is a flat plate equipped with a square insert panel. Different insert panels are tested: a smooth baseline surface and models with different arrays of circular cavities. The Reynolds number based on the momentum thickness is between 1440 and 3380.

The results evidence a thickening of the viscous sublayer with a consequent upward shift of the logarithmic region. The application of the VITA technique [1] reveals a reduction of the burst intensity (defined as the peak-to-peak value of the conditionally sampled streamwise velocity) as well as a shift of the peak of the burst frequency away from the wall. The burst frequency is shifted by $\Delta y^+ \cong 5$ and can be seen as a confirmation of the thickening of the viscous sublayer found in the mean velocity profile. From the PIV data a similar shift is evidenced in the production term of the turbulent kinetic energy budged. The quadrant analysis suggests that this is due to an increase in ejections and a decrease in the sweeps. The cavities then act similarly to most of the turbulent skin friction drag reduction techniques, for instance riblets and spanwise flow oscillations. These techniques disrupt the near wall turbulent cycle hence reducing the skin friction drag [2, 3].

In the full paper the effect of the geometrical parameters (cavity spacing and diameter) on the turbulent activity and on the drag reduction mechanism will be addressed.

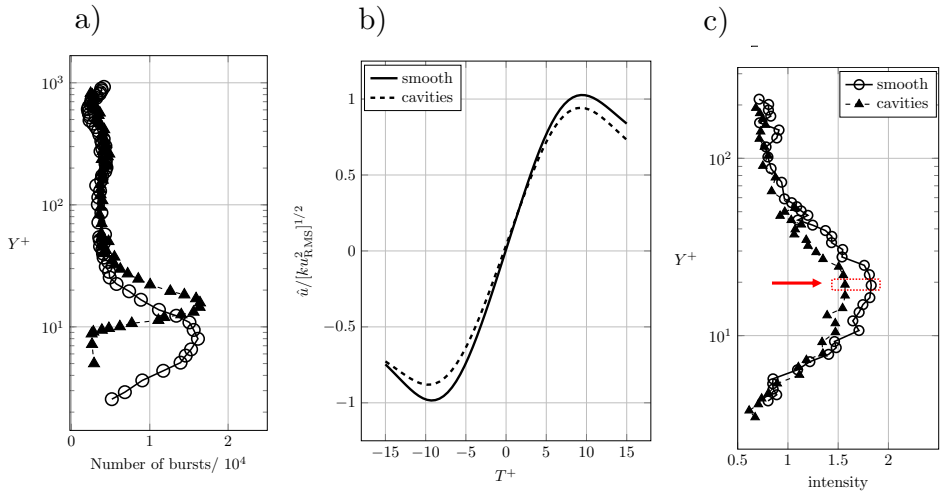

FIGURE 1. *a) Number of bursts profile, b) average burst signature for smooth and perforated, c) average burst intensity profile for smooth and perforated (results for $Re_\theta = 1440$)*

References

[1] R. F. Blackwelder and R. E. Kaplan, *On the wall structure of the turbulent boundary layer*, Journal of Fluid Mechanics **76** (1976), no. 1, 89–112.

[2] Ricardo García-Mayoral and Javier Jiménez, *Drag reduction by riblets*, Philosophical Transactions of the Royal Society A: Mathematical, Physical and Engineering Sciences **369** (2011), no. 1940, 1412–1427.

[3] Ivan Marusic, Dileep Chandran, Amirreza Rouhi, Matt fu, David Wine, Brian Holloway, Daniel Chung, and Alexander Smits, *An energy-efficient pathway to turbulent drag reduction*, Nature Communications **12** (2021).

[4] Pierre Ricco, Martin Skote, and Michael A Leschziner, *A review of turbulent skin-friction drag reduction by near-wall transverse forcing*, arXiv preprint arXiv:2103.04719 (2021).

INTERACTION OF TOLLMIEN-SCHLICHTING WAVES WITH FORWARD-FACING STEPS

M. Barahona[1], A. F. Rius-Vidales[1], F. Tocci[2], P. Ziegler[2,3], S. Hein[2] and M. Kotsonis[1]
[1] *Section of Aerodynamics, Delft University of Technology, Delft, The Netherlands.*
[2] *German Aerospace Center (DLR), Göttingen, Germany.*
[3] *University of Stuttgart, Stuttgart, Germany.*

Aerodynamic surfaces are subject to several spanwise-invariant irregularities which can promote early transition and a consequent increase in skin friction. A common surface irregularity is panel joints, which are usually preferred in a Forward-Facing configuration after several studies (e.g. [1]) proved that Backward-Facing steps have more detrimental effects on transition. Nevertheless, how a Forward-Facing Step (FFS) locally interacts with incoming Tollmien-Schlichting (TS) waves remains partially unknown. Prior investigations focused on establishing semi-empirical laws to describe the onset of transition based on several step parameters [2]. However, recent numerical results [3] signal important flow features at the step location, which might play a role in the subsequent growth of TS waves.

The present study concerns the close-examination of TS waves interaction with an FFS by means of experiments performed at TU Delft and Direct Numerical Simulations (DNS) conducted by DLR. Experimentally, the localised effect of the step on the incoming instabilities is determined using phase-locked Planar Particle Image Velocimetry (2C-2DPIV) and Hot-Wire Anemometry (HWA) measurements.

Figure 1 shows the distortion that TS waves undergo over a subcritical step ($\overline{h} = 732\ \mu m$). While both DNS and PIV show a similar TS wave distortion upstream and downstream of the step, important differences are evident in its immediate vicinity which could be associated to deviations from the nominal step geometry. This is observed for both u'- and v'-components (Figure 1 (a) and (b)).

In the workshop, the results for subcritical, critical and supercritical steps will be presented to show how the topological differences at the step are related to the explosive growth of TS waves downstream of the FFS. Additionally, Power Spectral Density results from HWA measurements will be included to track the changes in the disturbance energy distribution along the frequency domain as the TS waves encounter the step.

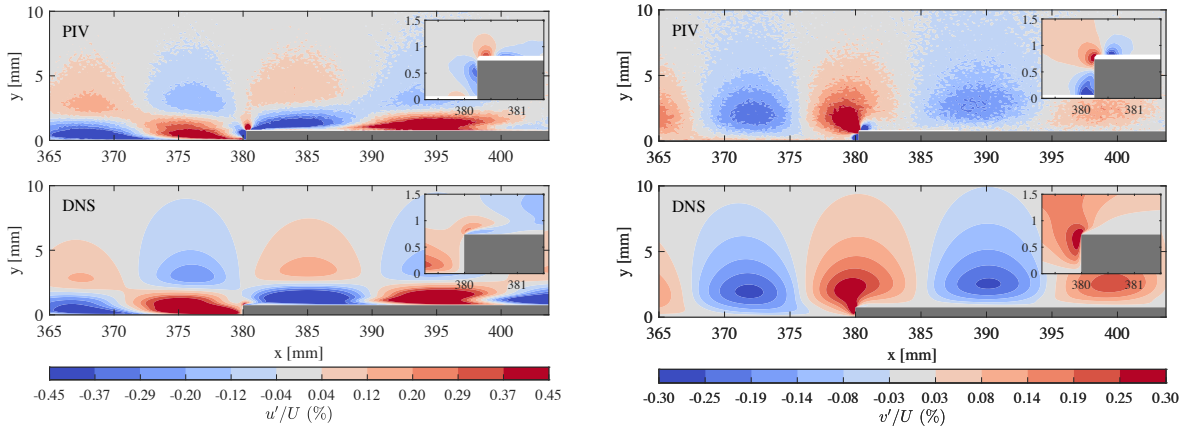

Figure 1: Contours of (a) streamwise and (b) wall-normal velocity fluctuations from phase-locked images measured with PIV and DNS flowfields at equivalent phase ($\varphi = 120°$), TS frequency (f = 450 Hz) and step height ($h/\delta^* = 0.775$). Contour limits from PIV and DNS zoomed images are magnified by four with respect to shown contour limits.

References

[1] Y. X. Wang and M. Gaster. 2005 Effect of surface steps on boundary layer transition. Experiments in Fluids, volume 39, pp. 679-686. Springer.
[2] A. Drake, A. Bender, A. Korntheuer, R. Westphal, W. Rohe, G. Dale, M. Gary, B. McKeon and S. Geraschchenko. 2010 Step excrescence effects for manufacturing tolerances on laminar flow wings. 48th AIAA Aerospace Sciences Meeting Including the New Horizons Forum and Aerospace Exposition.
[3] C. Edelmann, and U. Rist. 2014 Impact of forward-facing steps on laminar-turbulent transition in subsonic flows. In New Results in Numerical and Experimental Fluid Mechanics IX., pp. 155-162. Springer.

DNS OF THE INTERACTION OF CROSSFLOW INSTABILITIES WITH FORWARD-FACING STEPS

Francesco Tocci[1], Guillaume Chauvat[2], Alberto F. Rius-Vidales[3], Marios Kotsonis[3], Stefan Hein[1], Ardeshir Hanifi[2]

[1]*Institute of Aerodynamics and Flow Technology, German Aerospace Center (DLR), 37073 Göttingen, Germany*

[2]*FLOW Turbulence Lab., Department of Engineering Mechanics, KTH Royal Institute of Technology, SE-100 44 Stockholm, Sweden*

[3]*Section of Aerodynamics, Delft University of Technology, 2629HS Delft, The Netherlands*

Previous studies on the interaction between stationary crossflow (CF) vortices and a forward-facing step (FFS) have shown a significant influence on the laminar-turbulent transition (e.g. [1, 2]). In a recent experimental investigation, Rius-Vidales & Kotsonis [3] found that the effect of the step height on the transition location is non-monotonic. An unprecedented transition delay (w.r.t to the case without FFS) occurs when the incoming stationary CF vortices interact with a shallow FFS. Instead, the interaction with a higher FFS leads to an upstream advancement of the transition front location. The present work aims to numerically reproduce the experimental setup in [3] through direct numerical simulation (DNS). The current investigation's final goal is to understand further the flow physics behind the observed behaviour in the experiments.

The 3D DNS simulations are run on a relatively small domain to reduce the computational cost. The required boundary conditions for the latter are obtained with a complementary 2.5D RANS simulation followed by 2.5D DNS simulations for the base flow fields. The effect of discrete roughness elements used to condition the instability modes in the experiments is accurately reproduced via perturbations computed through nonlinear parabolised stability equations. Those are imposed at the inflow boundary of the 3D DNS domains. Unsteady noise is also added as a random forcing in the boundary layer such that the laminar-turbulent transition in the simulations approximates that in the experiments for the clean case without step.

The results show that the experimental setup can be numerically reproduced with sufficient accuracy as far as the steady flows are concerned, with a good agreement between the experimental and numerical velocity profiles upstream and downstream of the step. The transition delay effect due to a small FFS is also found in the DNS (Figure 1) and a detailed analysis of the unsteady disturbances will be presented to shed light on this behaviour.

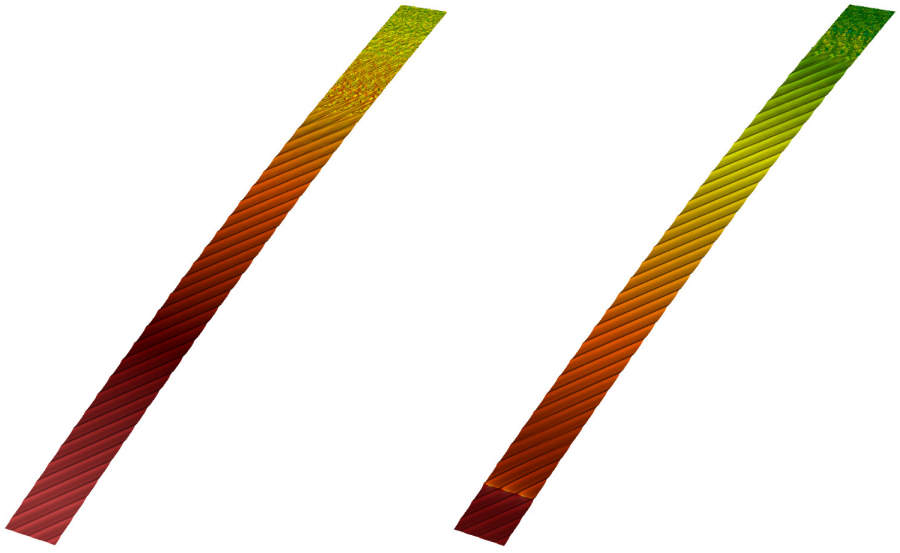

Figure 1: Isosurfaces of instantaneous magnitude velocity field colored by pressure in the clean case (left) and FFS case (right).

References

[1] J. L. Eppink. *Mechanisms of stationary cross-flow instability growth and breakdown induced by forward-facing steps. J. Fluid Mech.*, 897, A15, 2020.

[2] A. F. Rius-Vidales and M. Kotsonis. *Influence of a forward-facing step surface irregularity on swept wing transition. AIAA J.*, 58:12, 5243-5253, 2020.

[3] A. F. Rius-Vidales and M. Kotsonis. *Impact of a forward-facing step on the development of crossflow instability. J. Fluid Mech.*, 924, A34, 2021.

COLLECTIVE INSTABILITY OF A FLOW OVER STREAMWISE AND OBLIQUE RIBLET-LIKE ROUGHNESSES

A. Jouin[1,2], S. Cherubini[2], J.-C. Robinet [1]
[1] *DynFluid, ENSAM, 151, Bd. de l'Hôpital, 75013 Paris, France,*
[2] *DMMM, Politecnico di Bari, Via Edoardo Orabona, 4, Bari BA, Italy,*

Rough coatings represent an interesting technique for the possible reduction of drag or delay of the laminar-turbulent transition. However, stability analysis for these surfaces is often studied through homogenised Navier slip boundary conditions and the full geometry of the roughness is rarely considered in all its complexity. Following Ehrenstein [1], it could be taken into account through a coordinate change in the wall-normal direction. Unfortunately, due to the computational cost, the analysis remains usually restricted to the study of a single pattern together with periodic boundary conditions in the spanwise direction, potentially missing instability mechanisms spanning multiple iterations of the pattern. Schmid et al. [2] developed a framework that elegantly relax this constraint: considering a periodic system composed of multiple subunits, the block-circulant form of the linearised Jacobian matrix could be exploited to recast the problem into a much more numerically tractable form.

Thus, linear stability analysis in a channel flow with rough walls, and with the framework previously described, is investigated. Roughnesses considered are wave-like and square-like, eventually tilted at an angle θ with respect to the streamwise direction. As expected, linear stability appears strongly dependant of the geometry of the roughness: square-like riblets, with their sharp edges, are sensibly more unstable than the wave-like ones. In both cases, for streamwise riblets, the most unstable mode remains of the fully-periodic type, i.e with a fully synchronised motion. The full spectrum can be seen in Figure 1. On the contrary, transient growth seems dominated by unsynchronised motion at early times.

Orientation of the riblets has a deep impact on the stability of the flow: in the near-wall regions, shear-stress is not aligned anymore with the streamwise direction, thus creating cross-flow. In turn, this cross-flow, despite its small magnitude, seems responsible of the apparition of a new instability region, reminiscent of what could be observed in swept flows [3]. Interestingly, now, in both the modal and non-modal analysis, the unsynchronised motion seems to be prevalent, yielding both more unstable modes and higher energy growth.

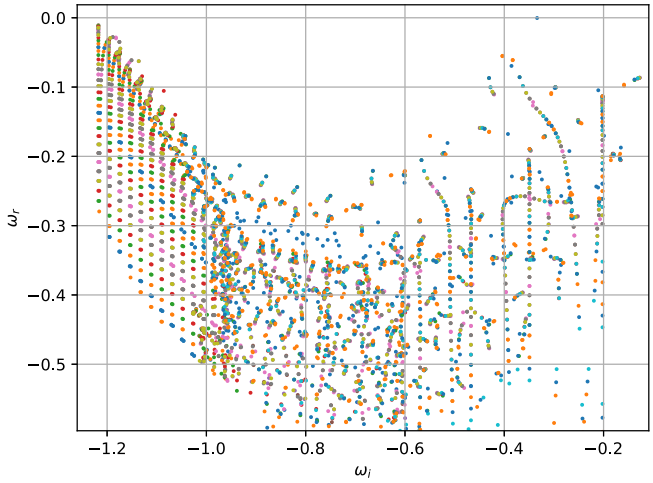

FIGURE 1. *Left: Spectrum for a 12-periodic array of wave-like streamwise roughnesses at* $Re = 5000$, $\alpha = 1.12$. *The least-damped mode is marginally stable and corresponds to a fully synchronised motion.*

References

[1] U. Ehrenstein. On the linear stability of channel flow over riblets. *Phys. Fluids*, 8 (11), 1996.
[2] P. J. Schmid, M. Fosas de Pando and N. Peake. Stability analysis for n-periodic arrays of fluid systems. *Phys. Rev. Fluids*, 2 (11), 2017.
[3] J. Serpieri. Cross-Flow Instability. TU Delft, 2018.

EXPERIMENTAL INVESTIGATION OF VORTEX STRUCTURES INDUCED BY A ROUGHNESS ELEMENT IN A BOUNDARY LAYER

Tristan M. Römer[1], Ulrich Rist[2]
[1] *University of Stuttgart, Pfaffenwaldring 21, D-70569 Stuttgart, Germany, roemer@iag.uni-stuttgart.de*
[2] *University of Stuttgart, Pfaffenwaldring 21, D-70569 Stuttgart, Germany, rist@iag.uni-stuttgart.de*

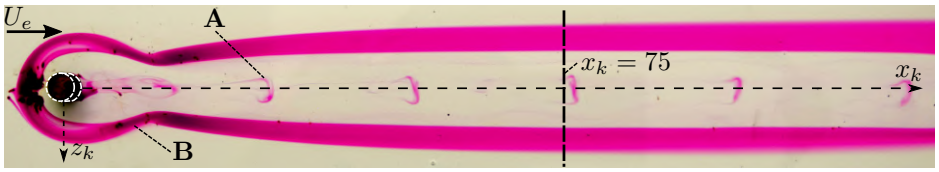

Looking at the vortex formation downstream of a cylindrical roughness element in a Blasius boundary layer, two major vortices can be found: a horseshoe and hairpin type [1][2]. The vortices are illustrated on the top (A: hairpin; B: horseshoe) by dye streakline visualization. The horseshoe vortex wraps around the cylinder and forms low-speed and high-speed streaks in the roughness element wake. If the Reynolds number exceeds a certain threshold value, hairpin vortices periodically separate from the top of the cylinder.

The present research focuses on the vortex motion and development of secondary structures behind the roughness element. The investigations are performed experimentally in the laminar water channel at the Institute of Aerodynamics and Gas Dynamics (IAG), where a steady 2-d laminar boundary layer forms on a flat plate. A cylindrical roughness element with height equal to width $d = k = 0.01\,\mathrm{m}$ (aspect ratio $\eta = d/k = 1$) is placed at the fixed position $x_k = x/k = 57$ behind the leading edge, where x_k represents the distance from the leading edge non-dimensionalized by k. The Reynolds number $Re_k = 770$ (supercritical) is based on k and the free-stream velocity U_e. The figure at the bottom left shows hydrogen bubble snapshots at $x_k = 75$ (see top figure) for different times $t_0 < t_1 < t_2$. At t_0, the hairpin head (A) can be clearly identified. In the next snapshot t_1, the head has passed and the hairpin legs are visible at $y_k = 1$. The hairpin is connected to a Λ-vortex (C) known from classical boundary layer transition (secondary instability). At t_2, another structure (D) can be seen, here named a V-vortex. The V-vortex is located between the Λ-vortex and the wall. It can be observed that Λ-vortex and V-vortex rotate in opposite directions. To identify the contribution of those vortices to laminar-turbulent breakdown, the fluctuation power measured by a hot-film probe is presented in the figure bottom right (same $x_k = 75$ position). The Λ-vortex (C) is the most dominant in terms of fluctuation power, while the V-vortex (D) has about 50% of the power of the Λ-vortex. Therefore, the V-vortex can be defined as a product of hairpin vortex motion and Λ-vortex rotation. The vortices seem to also be illustrated in [2]. The high fluctuation power of the the Λ-vortex indicates that it plays a key role in roughness induced laminar-turbulent breakdown.

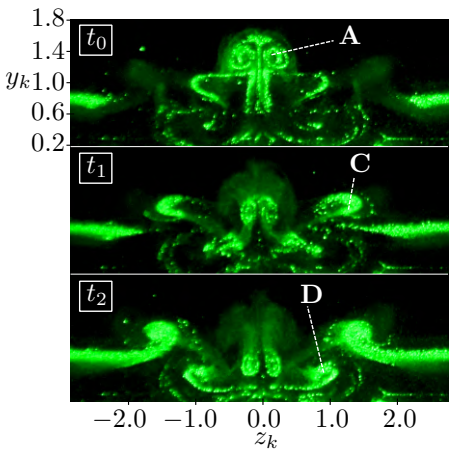

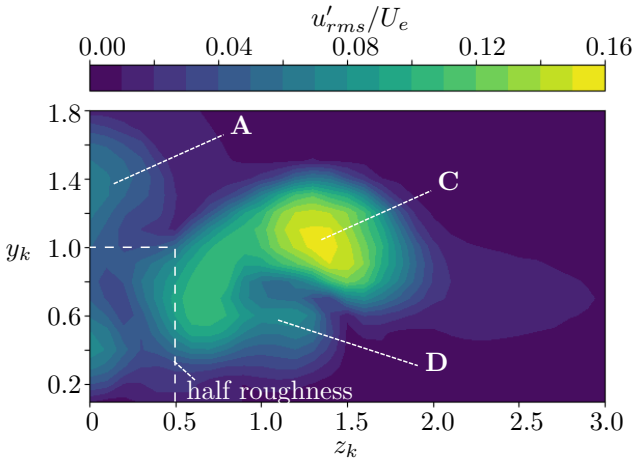

References

[1] M. S. Acarlar, C. Smith. A study of hairpin vortices in a laminar boundary layer. Part 1. Hairpin vortices generated by a hemisphere protuberance. *J. Fluid Mech.*, 175, 1-41, 1987

[2] J. Loiseau, J. Robinet, S. Cherubini and E. Leriche. Investigation of the roughness-induced transition: global stability analyses and direct numerical simulations. *J. Fluid Mech.*, 760, 175-211, 2014

ROTATING WALL-NORMAL CYLINDRICAL ROUGHNESS ELEMENTS INDUCED BOUNDARY LAYER TRANSITION

Yongxiang Wu[1], Tristan Römer[1], Gabriel Axtmann[1], Ulrich Rist[1]
[1]*Institute of Aerodynamics and Gas Dynamics, University of Stuttgart, Pfaffenwaldring 21, D-70569 Stuttgart, Germany*

Velocity streaks induced by cylindrical roughness elements are found to be capable of attenuating Tollmien-Schlichting (TS) instabilities and delaying transition [2]. The underlying mechanism is due to the induced negative spanwise production of perturbation kinetic energy [1]. In a previous study [3], the TS-waves are found to be effectively stabilized by a special setup with rotating cylindrical roughness elements as well, as shown in figure 1(a). The rotation rate is $\Omega_u = \Omega D/2u_k$, here Ω is the angular velocity of the cylinder, D the cylinder diameter and u_k the unperturbed Blasius velocity at the upper edge of the cylinder.

The present study investigates the induced boundary layer transition with Direct Numerical Simulations (DNS), Dynamic Mode Decomposition (DMD) and Perturbation Kinetic Energy (PKE) analysis. The laminar base flow is calculated with a selective frequency damping (SFD) solver, examples for $\Omega_u = 0.0$ and 1.0 are shown in figure 1(b,c). The wake of a rotating cylindrical roughness element is featured by a strong DIV surrounded by a SIV.

An increase of the rotation speed Ω_u results in a supercritical Hopf bifurcation. Below $\Omega_u < 0.65$, the boundary layer is subjected to convective instability. While above $\Omega_u > 0.65$, a self-sustained global instability is observed. With $0.65 < \Omega_u \leq 0.75$, the global instability is initiated by a combination of elliptical and centrifugal instabilities in the near wake. With $0.75 \leq \Omega_u \leq 1$, Taylor-Couette-like streamwise vortices are generated on the decelerated side, which then create a protruding reverse-flow region. In the near wake, the mechanism gradually changes to a pure centrifugal instability as rotation speed increases. For further increasing Ω_u, the onset of global instability is directly located on the decelerated side of the cylinder stubs, where a deceleration mechanism feeds the instability by extracting energy from the mean-flow. The example of case $\Omega_u = 1.31$ is shown in figure 2. Beyond $\Omega_u \geq 1.375$, the flow becomes chaotic.

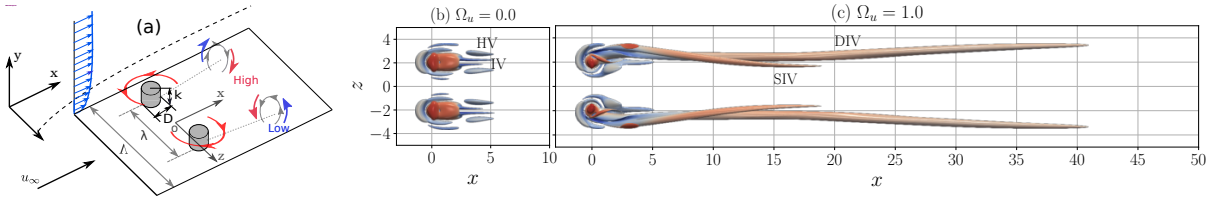

FIGURE 1. *Numerical set-up and Vortex visualization for case $\Omega_u = 0$ and $\Omega_u = 1$. HV: horseshoe vortex, IV: inner vortex, DIV: dominating inner vortex, SIV: secondary inner vortex.*

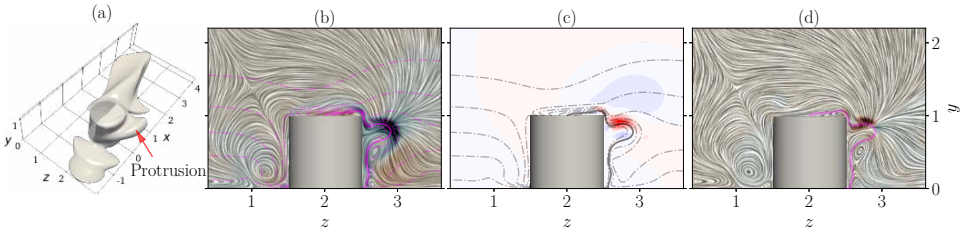

FIGURE 2. *(a): Reversed flow regions by meanflow $\bar{u} = 0$ isosurfaces, (b): Streamwise vortices at $x = 0$, colored by streamwise gradient $\partial\bar{u}/\partial x$, (c): Real part of leading DMD mode in $x = 0$ plane, (d): Total local energy production $\sum I_i$ at $x = 0$. Thin dashed lines are isolines of $\bar{u} = -0.2, 0.2, 0.4, 0.6, 0.8, 0.95$, thick solid line marks $\bar{u} = 0$.*

References

[1] C. Cossu and L. Brandt. *On Tollmien–Schlichting-like waves in streaky boundary layers*, *Eur. J. Mech. B Fluids*, 23(6):815-833, 2004
[2] JHM. Fransson and A. Talamelli and L. Brandt and C. Cossu. *Delaying transition to turbulence by a passive mechanism Phys. Rev. Lett.*, 96(6) 064501, 2006.
[3] Y. Wu, G. Axtmann, U. Rist. *Linear stability analysis of a boundary layer with rotating wall-normal cylindrical roughness elements. J. Fluid Mech.*, 915, 2021.

LAMINAR FEEDBACK MECHANISMS OF JET TONE GENERATION

Flavio Giannetti[1], Javier Sierra[1,2], David Fabre[2], Vincenzo Citro[1], Paolo Luchini[1]
[1] *University of Salerno, Via Giovanni Paolo II, 84084 Fisciano (SA) Italy*
[2] *Institut de Mecanique des Fluides de Toulouse, 2 All. du Professeur Camille Soula, 31400 Toulouse, France*

It is well known that jets, under particular conditions, may generate intense tonal noise. In many cases, the sound is produced by the action of a self-excited instability. In this presentation we review two different configurations where this occurs: the case of a jet impinging on a wall and the case of a jet passing trough a circular aperture of finite thickness. In the first case it is generally accepted [1, 2] that intense tones can be produced by a non-local feedback loop among two kinds of waves: a downstream-travelling wave, which is excited at the nozzle lip and propagates around the jet core position, and an upstream-travelling wave generated by the reflection of the first wave on the plate which propagates backward inside the jet core. The interaction of such waves gives rise to a self-sustained global instability, which in some circumstances is able to radiate an intense acoustic field. In the presentation we will review the characteristics of the self-sustained mechanism in the laminar regime and its noise radiation by using both a global and a local analysis that will precisely identify the components of the feedback mechanism. The case of the jet passing through a circular aperture will be analysed by an approach based on impedance [3, 4]. It will be shown that the knowledge of the global impedance provides an instability criterion and a prediction of the eigenvalues of the full system. Two generic situations will be considered. In the first one, the upstream domain is a closed cavity while the downstream domain is open, leading to a class of conditionally unstable modes. In the second situation, the two regions, upstream and downstream of the hole are considered as open, leading to a class of hydrodynamic modes where the instability of the recirculation region is sufficient to generate self-oscillations without the need of any resonator. A matched asymptotic model, valid in the low-Mach limit, is then used to derive a global impedance of the system, combining the impedance of the hole and of both upstream and downstream domains. The accuracy and validity of the proposed approach will be assessed by comparing the results with those obtained from the linearised fully compressible formulation.

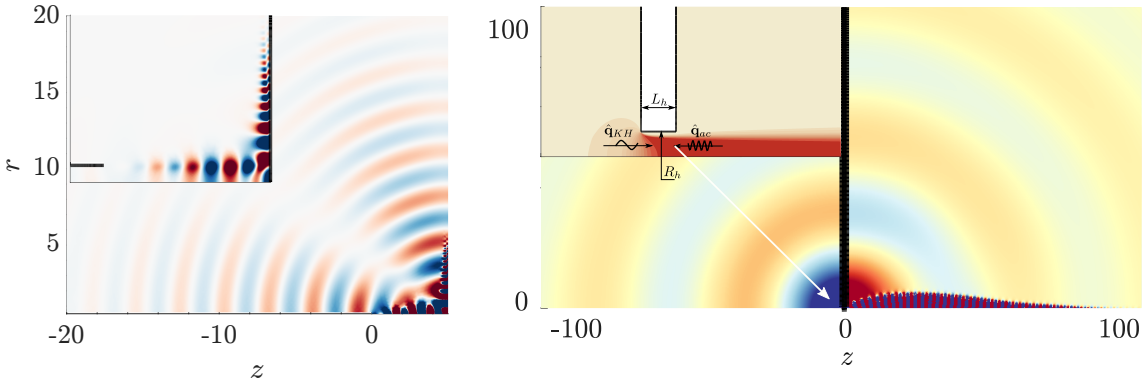

Figure 1: Real part of the pressure component of the critical modes. (a) Compressible rounded impinging jet for an averaged Mach number at the inlet of $M = 0.6$. (b) Hole tone configuration for a ratio $\beta = L/R_h = 2$ (inset in the upper left corner) for an averaged Mach number at the hole of $M = 0.05$.

References

[1] V. Jaunet, M. Mancinelli, P. Jordan, A. Towne, D. Edgington-Mitchell, G. Lehnasch and S. Girard1 Dynamics of round jet impingement *Proceedings of 25th AIAA/CEAS Aeroacoustics Conference and Exhibit, 20-23 May 2019, Delft, The Netherlands 25th AIAA/CEAS Aeroacoustics Conference*, 2019.
[2] G. Camerlengo, J. Sesterhenn, F. Giannetti, V. Citro and P. Luchini. On the Stability of Subsonic Impinging Jets *Proceedings of the Conference of the Italian Association of Theoretical and Applied Mechanics*, 2019.
[3] J. Sierra, D. Fabre, V. Citro, and F. Giannetti. Acoustic instability prediction of the flow through a circular aperture in a thick plate via an impedance criterion. *J. Fluid Mech.*, accepted, 2022.
[4] D. Fabre, R. Longobardi, V. Citro, and P. Luchini. Acoustic impedance and hydrodynamic instability of the flow through a circular aperture in a thick plate. *J. Fluid Mech.*, 885, 2020.

EFFECT OF LEWIS NUMBER ON THE LINEAR STABILITY OF JET FLAMES

Christopher Douglas[1], Wolfgang Polifke[2] and Lutz Lesshafft[1]
[1] *LadHyX, Ecole Polytechnique, 91128 Palaiseau Cedex, France*
[2] *Mechanical Engineering Department, TU Munich, Boltzmannstr. 15, D-85747 Garching, Germany*

Ongoing concerns about combustion-related greenhouse gas emissions have motivated substantial efforts towards integrating carbon-free alternative fuels such as hydrogen (H_2) into existing energy infrastructure. Nonetheless, H_2 is characterised by remarkably high mass diffusion rates (low Lewis numbers), giving its flames extreme sensitivity to stretch effects and thermal-diffusive instability [1]. These flame dynamics are also intimately coupled to the hydrodynamic properties of the flow within which the flame is embedded [2]. While these flame and flow dynamics are both mature areas of research when considered separately, relatively little is known about their behaviour when coupled interactions are included.

To this end, we investigate the modal and nonmodal linear global stability of laminar, lean-premixed Bunsen jet flames across a range of Lewis numbers from $Le = 0.5$ to $Le = 1$. The system is described using a fully coupled low Mach number formulation of the compressible Navier-Stokes equations with a single-step, irreversible Arrhenius chemistry model. Our results provide insight into the effect of thermal-diffusive instability on the coupled flame and flow dynamics, with clear implications toward H_2 combustion systems.

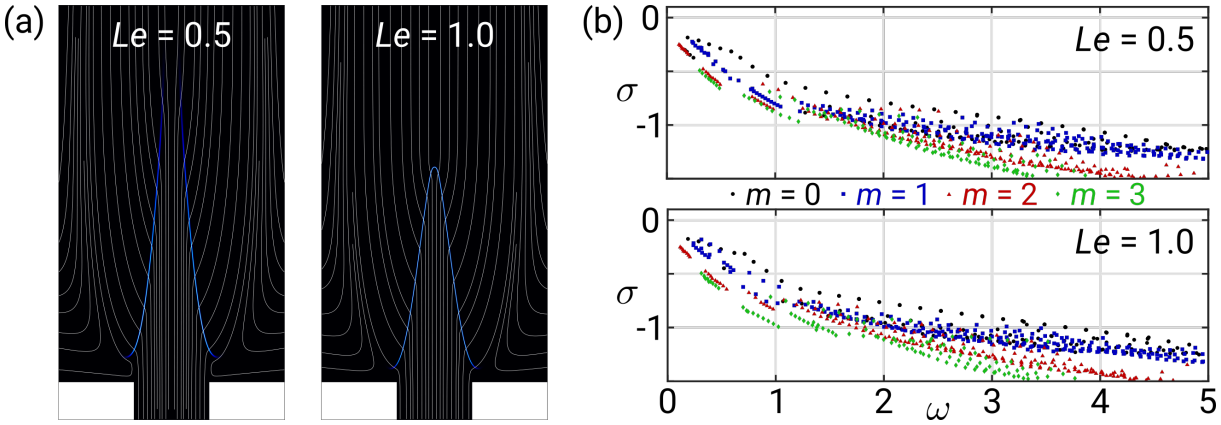

FIGURE 1. *Steady flame shapes visualised by reaction rate contours and (b) corresponding global eigenspectra for indicated azimuthal wavenumbers m.*

References

[1] J. Beita and M. Talibi and S. Sadasivuni and R. Balachandran. Thermoacoustic Instability Considerations for High Hydrogen Combustion in Lean Premixed Gas Turbine Combustors: A Review. *Hydrogen*, 2(1):33–57, 2021.
[2] M. Meindl and C. F. Silva and W. Polifke. On the spurious entropy generation encountered in hybrid linear thermoacoustic models. *Combustion and Flame*, 223:525–540, 2021.

A COMPUTATIONAL FRAMEWORK FOR LINEAR ANALYSIS OF LARGE-SCALE N-PERIODIC SYSTEMS

Athanasios T. Margaritis[1], Taraneh Sayadi[2], Olaf Marxen[3], Peter J. Schmid[4]
[1] *PhD Candidate, Dept. of Mathematics, Imperial College London, SW7 2AZ, London, United Kingdom*
[2] *CNRS Researcher, Institut Jean-le-Rond d'Alembert, Sorbonne University, 75252, Paris, France*
[3] *Lecturer, Dept. of Mech. Eng. Sciences, University of Surrey, GU2 7XH, Guildford, United Kingdom*
[4] *Professor, Faculty of Mechanical Engineering, KAUST, 23955, Thuwal, Kingdom of Saudi Arabia*

This work is focused on the application of the mathematical framework presented in [1] for the linear analysis of n-periodic flow systems. The methodology is extended and applied to relevant large-scale problems. We present a minimally intrusive implementation for large-scale flow solvers where explicit access to the underlying matrix operators is typically unavailable. A demonstration is done using an in-house, high-fidelity direct numerical simulation (DNS) high-order compact finite-differences solver. The necessary theoretical background is described, based on a set of complex numbers called the *roots of unity*, $\rho_j = \exp(2\pi ji/n),\ j = 0, 1, \ldots, n-1$. The capability to dissect a large problem into a number of smaller, fully decoupled problems is emphasised. This is done by reducing the n-periodic system to a triplet of units, and studying the sub-problem while varying the root-of-unity parameter. This allows for massive parallelisation and meaningful insight without significant computational overhead. From such sets of simulations of triplets it is straightforward to access information regarding the linearised response of the full configuration of n units for an arbitrary number n, covering a larger range of dynamics compared to the typical choice of a single unit with periodic boundaries. It is thus possible to approximate the underlying linear interactions and synchronisations of the cross-unit dynamics at a reduced computational cost. The methodology is demonstrated for systems of n-periodic surface irregularities in boundary layers where there is potential for cross-unit interactions and synchronisation of the smaller-scale dynamics into larger-scale structures. Such examples include spanwise arrays of jet injections or roughness elements in a boundary layer. The proposed framework can provide relevant insight into the effects of synchronisation and linear cross-unit interactions in such cases. The efficiency and fidelity of the methodology, and the capability to implement it in a minimally intrusive manner in a variety of solvers, suggest it can be a valuable tool for sensitivity analysis and fine-tuning, or early-design studies when there is a need to investigate various configurations.

References

[1] P. J. Schmid, M. Fosas de Pando, and N. Peake. Stability analysis for n-periodic arrays of fluid systems. *Physical Review Fluids*, 2(11):7739-7755, 2017.

INVISCID LINEAR AND NONLINEAR DYNAMICS OF VISCOSITY STRATIFIED SHEAR LAYERS OF ONE FLUID SURROUNDED BY ANOTHER FLUID

Juan-Ángel Tendero-Ventanas[1], Saikishan Suryanarayanan[2], Sharath Jose[3], Vassilios Theofilis[4,5], Rama Govindarajan[3]

[1] *Universidad de Cádiz, Puerto Real, Spain.*
[2] *The University of Texas at Austin, Austin TX, United States of America.*
[3] *International Centre for Theoretical Sciences, Bengaluru, India.*
[4] *School of Engineering, University of Liverpool, United Kingdom.*
[5] *Escola Politecnica, University of São Paulo, Brasil.*

Linear and nonlinear evolution of three viscosity stratified shear layers are studied using linear stability analysis, Lagrangian vortex calculations and direct numerical simulations. [1, 2] studied the flow in a viscous shear layer and in the flow past an incline respectively. The present idea is to pare down the physics to its simplest form, and study a three layer flow, where a thin layer of one fluid is surrounded by other fluid above and below, all sheared from top and bottom, see Figure 1.

Two scenarios are studied, one where the middle fluid has half of the viscosity of the outer fluid, and one where it is double. The first case is found to be modally unstable, while the second is stable, but can experience high values of transient growth.

In both cases, the results show that the primary role of viscosity stratification is to create a vorticity stratification and that the subsequent instability and nonlinear evolution can be understood from 2D inviscid dynamics.

For the unstable case, the initial evolution of random perturbations in inviscid Lagrangian vortex simulations follows the predictions of linear stability theory and the subsequent evolution is studied and understood in terms of a free shear layer roll-up modified by a background shear. Direct numerical simulations with viscosity stratification performed using Gerris with matched initial conditions show (Figure 2) nearly identical evolution with the inviscid simulation for wide ranges in viscosity (Reynolds number ranging from 400 to 10000) and diffusion (Schimdt number ranging from 0.05 to ∞) suggesting the strongly inviscid nature of the underlying dynamics of this viscosity stratified flows. Three dimensional viscous simulations also show that there are many scenarios where three dimensionality can be disregarded.

The configuration where the vorticity stratification leads to the modally stable case exhibits a novel transient growth mechanism, which is partly observed in the viscous simulations, but is affected and damped by viscosity.

A new configuration where inviscid mechanisms are behind instabilities in sheared flow is exposed here. This research aims to extend the idea of the inviscid nature of such instabilities by the comparison of inviscid and viscous simulations at a variety of Reynolds numbers.

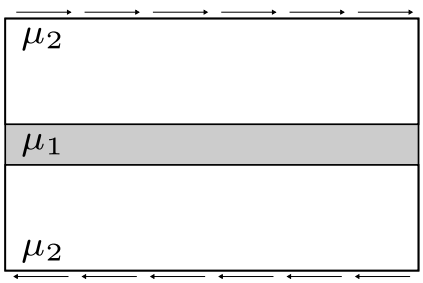

Figure 1: Schematic of the layout, central layer of viscosity μ_1 surrounded by fluid with viscosity μ_2.

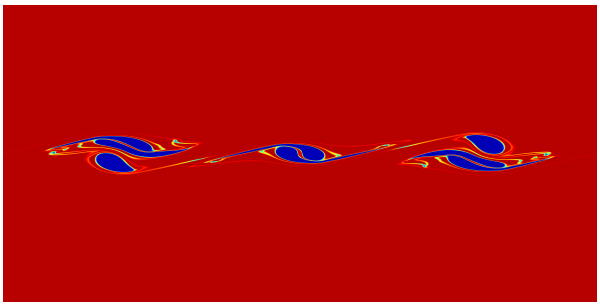

Figure 2: Snapshot at time 64 of the nonlinear evolution for the viscous simulation, where vortex roll-up is observed. Blue is fluid 1 and Red fluid 2.

References

[1] K. C. Sahu, and R. Govindarajan. Instability of a free-shear layer in the vicinity of a viscosity-stratified layer. *Journal of fluid mechanics*, 752:626–648, 2014.

[2] S. Ghosh, R. Usha, R. Govindarajan, and O. Tammisola. Inviscid instability of two-fluid free surface flow down an incline. *Meccanica*, 52:955–972, 2017.

AEROELASTIC AND RADIATIVE INSTABILITIES ON A TENSIONED MEMBRANE PLACED UNDER A FREE SURFACE

Nabil Achour[1], David Fabre[1] & Jérôme Mougel[1]
[1] *IMFT, University of Toulouse*

We consider the stability properties of a tensioned membrane of finite length L located at the bottom of a fluid layer of depth h, in presence of a uniform incoming current. This configuration, referred to as the *Nemtsov membrane*, is known to be affected by two possible kinds of instabilities. The first are *aeroelastic instabilities*, related to the instabilities existing in the "flag" configuration [3, 4], which exist even in the absence of a free surface. The second ones are *radiative instabilities*, and are related to the possibility for the system to be destabilized by surface wave radiation. More specifically, such instabilities are a direct consequence of the existence of negative energy waves (neWs), and were first evidenced in the shallow-water limit, and in the supercritical range ($Fr > 1$) [5, 2]. In this presentation we will draw a parametric map of the ranges of existences of these instabilities as function of the four nondimensional parameters appearing in the problem, namely the Froude number Fr comparing flow velocity to surface wave velocity, the reduced depth h/L, the mass ratio α and the reduced velocity U_r comparing flow velocity to membrane wave velocity. In strongly coupled cases, we extend results by [4, 1], to finite length membranes and explore the intricate stability characteristics of the system. We also show that radiative instabilities also exist in the subcritical régime thanks to the dispersive nature of waves in the finite-depth case. It is also shown that aeroelastic instabilities of both divergence (static instability) or flutter (dynamic instability) kinds emerge and are affected by the free surface, and that such instabilities coexist with radiative instabilities.

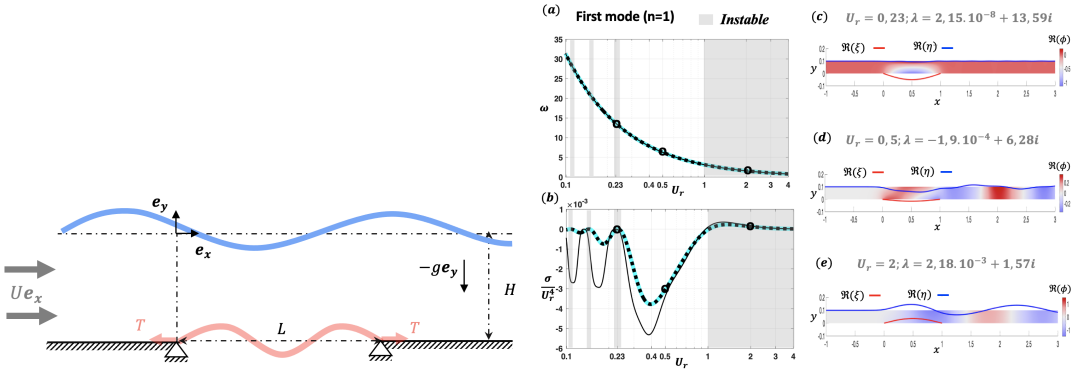

FIGURE 1. (*left*) *Sketch of the Nemtzof membrane configuration;* (*right*) *Frequencies, amplification rates, and mode structure for the radiative instablities associated to first structural mode for* $\alpha = 10^{-2}$, $h = 0.1$, *and* $Fr = 2$.

References

[1] Joris Labarbe and Oleg N Kirillov. Membrane flutter induced by radiation of surface gravity waves on a uniform flow. *Journal of Fluid Mechanics*, 901, 2020.
[2] Joris Labarbe and Oleg N Kirillov. Radiation-induced instability of a finite-chord nemtsov membrane. *arXiv preprint arXiv:2104.01060*, 2021.
[3] Sébastien Michelin and Olivier Doaré. Energy harvesting efficiency of piezoelectric flags in axial flows. *Journal of Fluid Mechanics*, 714:489–504, 2013.
[4] Jérôme Mougel and Sébastien Michelin. Flutter and resonances of a flag near a free surface. *Journal of Fluids and Structures*, 96:103046, 2020.
[5] BE Nemtsov. Flutter effect and emission in the region of anomalous and normal doppler effects. *Radiophys. Quantum Electron.(Engl. Transl.);(United States)*, 28(12), 1986.

TRANSITION PREDICTION IN THREE-DIMENSIONAL FLOWS WITH THE HARMONIC LINEARIZED NAVIER-STOKES EQUATIONS

Pedro Paredes[1], Meelan Choudhari[2], Mark H. Carpenter[2], and Fei Li[2]
[1]*National Institute of Aerospace, Hampton, VA 23666, USA.*
[2]*NASA Langley Research Center, Hampton, VA 23681, USA.*

The conventional method to predict the onset of laminar-turbulent transition in convectively unstable boundary-layer flows is based on the logarithmic amplification ratio, the so-called N-factor, of the linear instability waves. To calculate the N-factor, the flow variables are decomposed into a laminar basic state solution and the linear disturbances, which are assumed to be harmonic in time. The most commonly used linear stability analysis approaches include the locally parallel linear stability theory (LST) and the non-local, weakly nonparallel parabolized stability equations (PSE). However, these methods do not account for strong streamwise gradients that are encountered in several configurations of interest, as roughness elements, steps, gaps, or corners. To solve the linear evolution of disturbances along such strongly non-parallel regions, the harmonic linearized Navier-Stokes equations (HLNSE) need to be solved [1]. The discretization of the HLNSE for spanwise/azimuthally inhomogeneous laminar basic states yields a linear system of complex arithmetic with a leading dimension of the order of 10^7 to 10^8 for many problems of current interest in NASA applications. A combined multithread and multiprocessor algorithm based on the Thomas' algorithm and the dual Schur complement method is implemented for the direct solution of such linear system. This algorithm reduces the scaling of the cpu time and memory requirements with respect to the number of streamwise points from cubic to linear and from quadratic to linear, respectively.
A combination of the PSE and HLNSE is used to study the evolution of linear disturbances over a flat plate with a sinusoidal roughness path at freestream unit Reynolds number of 12.6×10^6 m^{-1} and Mach 3.5 to support an experimental campaign [2]. The evolution of the 80 kHz AA disturbance, i.e., with antisymmetric boundary conditions in both symmetry planes, is shown in Fig. 1(a). The favorable agreement with the measured power spectra in Fig. 1(b) confirms the significance of disturbance growth over the roughness patch and the effect on the instabilities in the wake.
This material is based upon research supported by the Hypersonic Technology Project (HTP) and the NASA Transformational Tools and Technologies (TTT) project of the Transformative Aeronautics Concepts Program under the Aeronautics Research Mission Directorate.

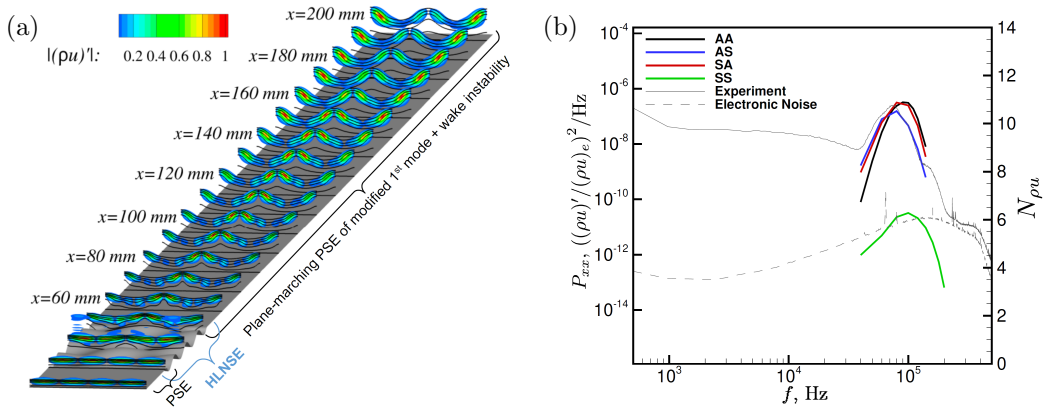

FIGURE 1. *(a) Streamwise mass flux contours of 80 kHz disturbance and basic state isolines over the rough plate at Mach 3.5. (b) Comparison of power spectra to most-amplified disturbances at* 153.8 *mm distance from the leading edge. The disturbance evolution is calculated with a combination of PSE and HLNSE. Reproduced from Ref. [2]*

References

[1] M. Choudhari, and C. Streett. Theoretical prediction of boundary-layer receptivity. AIAA Paper 94-2223, 1994.
[2] A. Chou, P. Paredes, M. Kegerise, R. King, M. Choudhari, and F. Li Transition Induced by an Egg-Crate Roughness on a Flat Plate in Supersonic Flow. *J. Fluid Mech.*, submitted, 2022.

AN EFFICIENT HARMONIC NAVIER-STOKES SOLVER FOR NON-LINEAR STABILITY PROBLEMS IN COMPLEX DOMAINS

S. Westerbeek[1], J. Casacuberta[1], M. Kotsonis[1]
[1] *TU Delft, Leeghwaterstraat 42, 2628 CA Delft,* *S.H.J.Westerbeek@tudelft.nl*

The laminar-to-turbulent transition of boundary layers is known to be significantly affected by complex geometrical features, such as steps, humps, and gaps. Yet, classical stability theory approaches such as Orr-Sommerfeld eigenvalue analyses or Parabolised Stability Equations are unable to model these cases by virtue of the underlying assumptions [1]. This necessitates the use of fully elliptical approaches such as Direct Navier-Stokes (DNS) simulations, which nevertheless are extremely resource- and time-intensive. An alternative and efficient compromise between simplified approaches and a full DNS can be gained by considering a harmonic expansion of the Navier Stokes (NS) equations in the temporal and spanwise spatial dimension [2, 3]. Based on these approaches, an efficient harmonic NS solution algorithm is developed that can model non-linear stability problems while accounting for complex geometrical features.

The incompressible generalized Harmonic Navier-Stokes (HNS) equations are used in a perturbed formulation where velocity and pressure are decomposed into a steady (Q) and fluctuating (q') component. For all quantities, the perturbation ansatz yields

$$q'(x,y,z,t) = \sum_m \sum_n \hat{q}_{m,n}(x,y) e^{\mathrm{i}(\beta_n z - \omega_m t)} + \text{c.c}, \quad \beta, \omega \in \mathbb{R}; \quad \hat{q} \in \mathbb{C}, \tag{1}$$

where $\hat{q} = [\hat{u}, \hat{v}, \hat{w}, \hat{p}]^T$, $\mathrm{i} = \sqrt{-1}$, β the spanwise wavenumber, ω the angular frequency, "c.c" the complex conjugate, t is time and x, y, z represent the streamwise, wall-normal and spanwise directions respectively. Spanwise invariance in the base flow is assumed. The discretization is performed by a fourth-order central finite difference scheme in the streamwise direction and spectral differentiation in the wall-normal direction. Smooth geometrical features are accounted for by using a generalized curvilinear domain transformation. Sharp features are modeled using a domain-embedded no-slip condition. The continuity equation is solved directly as an implicit equation for pressure. Non-linear terms are solved explicitly using harmonic balancing. The combined discretized system is solved using a direct sparse solver.

In this work, the solution to the non-linear HNS equations will be compared with DNS for representative cases in unswept and swept-wing boundary layers, respectively governed by the evolution of Tollmien-Schlichting and Crossflow Instabilities. Results will be presented in complex domains entailing forward-facing steps for three different step heights and a range of incoming disturbance amplitudes.

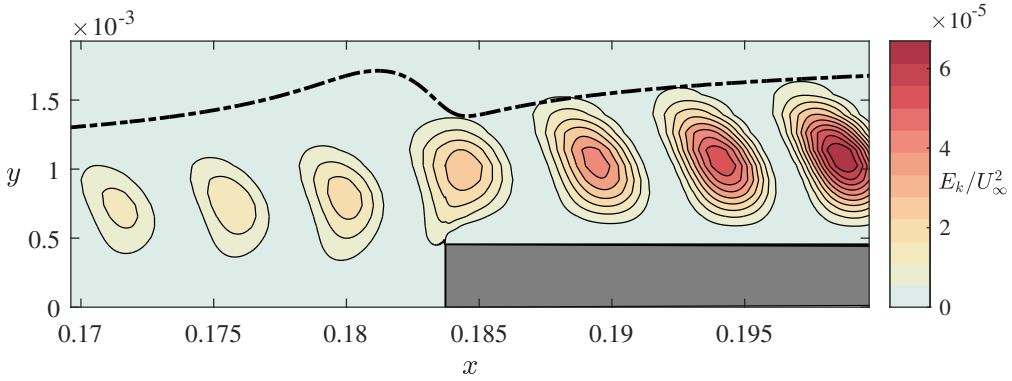

FIGURE 1. *Perturbation kinetic energy contours in the near-step region for an incoming stationary crossflow disturbance. The step is indicated by the gray rectangle and the dash-dotted line indicates the δ_{99} of the base flow.*

References

[1] Bertolotti, F. P., Herbert, T. & Spalart, P. R. Linear and nonlinear stability of the Blasius boundary layer. *Journal of fluid mechanics, 242, 441-474,* 1992.
[2] Franco Sumariva, J. A. & Hein, S. Adaptive Harmonic Linearized Navier-Stokes equations used for boundary layer instability analysis in the presence of large streamwise gradients. *2018 AIAA Aerospace Sciences Meeting (p. 1548),* 2018.
[3] Streett, C. Direct harmonic linear Navier-Stokes methods for efficient simulation of wave packets. *36th AIAA Aerospace Sciences Meeting and Exhibit (p. 784),* 1998.

NEKSTAB: A COMPLETE OPEN-SOURCE STABILITY ANALYSIS FRAMEWORK FOR NON-HOMOGENEOUS STEADY AND TIME-PERIODIC INCOMPRESSIBLE FLOWS

R. A. S. Frantz, J.-Ch. Loiseau and J.-Ch. Robinet[1]
[1] *DynFluid, Arts et Métiers Paris, 151 Boulevard de l'Hôpital, 75013 Paris*

With the massive increase in computational power over the past three decades, the focus of hydrodynamic stability research has shifted from local analyses based on the assumption of parallel flow to fully three-dimensional flows such as the roughness-induced boundary layer flow. It should be emphasised, however, that most recent work has been concerned with the stability of stationary base flows, while the modal and non-modal stability of time-periodic flows has attracted much less attention. Time-periodic flows rise due to forcing (e.g., forced coaxial jet) or naturally as they pass through a Hopf bifurcation (i.e., flow past one or two cylinders). To uncover the physical origin of modes or the receptivity of a given disturbance in periodic flow with no homogeneous directions in space, one can follow the linear evolution of infinitesimal perturbations evolving near limit cycles using the fully three-dimensional Navier-Stokes equations. Before doing so, however, unstable time-periodic solutions (also known as limit cycles) need to be numerically computed. Computation of such unstable limit cycles has traditionally been achieved by imposing existing spatiotemporal symmetries in combination with Newton-like methods, which are usually restricted to two-dimensional problems. A new implementation of a Newton-Krylov algorithm based on a GMRES method is capable of computing steady and periodic states of fully three-dimensional flows. When linearized around such time-periodic solutions, the resulting non-autonomous Navier-Stokes operator accepts solutions following Floquet theory, with the stability being characterised by Floquet exponents. Due to the high number of degrees of freedom required to adequately discretize these problems, the effect of the time-periodic Jacobian matrix on a given vector is computed in a time-stepping fashion, and the eigenvalue problem solved using an Arnoldi-based algorithm. Our framework relies on the highly parallel spectral element solver Nek5000. We introduce an open-source toolbox named NekStab based on Krylov methods to tackle stability problems based on the spectral element solver Nek5000. We present techniques built on the Nek5000 platform as well as validations and new cases involving both free and forced time-periodic flows, including secondary instabilities and the bifurcations experienced in the wake of bluff bodies.

ADJOINT-BASED OPTIMAL CONTROL OF SHARP INTERFACE MULTIPHASE FLOWS

Alexandru Fikl and Daniel J. Bodony
Department of Aerospace Engineering
University of Illinois at Urbana-Champaign

Multiphase phenomena are ubiquitous in many engineering applications and significant effort has been invested in understanding and optimizing such systems. While modeling and numerical simulation of multiphase flows have made impressive headway in the last two decades, much less can be said about the control of multiphase systems. Many practical control applications are based on experience and trial-and-error methods due to the large dimensionality of the problem, complexity of the coupled phases, and difficulty in developing reduced-order models from experimental data.

We leverage progress made in simulation-based predictions of the fluid dynamics of multiphase flows by developing and implementing a continuous adjoint formulation for incompressible, immiscible two-phase viscous flows with surface forces. The general formulation has been recently developed for flows with arbitrary Reynolds and Capillary numbers [1]. A Stokes-limit specialization has also been developed [2, 3, 4]. Both formulations support adjoint-based gradients for time-dependent cost functionals defined on the interphase surfaces and in the volume.

A specific example application of the theory is sketched in Fig. 1 where the optimal far-field velocity boundary conditions are sought such that an isolated, initially spherical drop traverses a specified curve in the $z = 0$ plane. The objective function being minimized is the tracking functional

$$\mathcal{J} = \frac{1}{2}\int_0^T \int_{\Sigma(t)} ||\vec{X} - \vec{X}_d||^2 \,\mathrm{d}\mathcal{S}\,\mathrm{d}t, \tag{1}$$

which measures the difference between the actual droplet surface $\vec{X}(t)$ and the target spherical droplet surface $\vec{X}_t(t)$ whose center of mass follows the red curve in Fig. 1. The decrease in Eq. (1) is given in Fig. 2. Observe that $\min \mathcal{J} > 0$ because the droplet cannot remain spherical due to its motion.

The contributed paper will include the formulations, their implementations and their application to several demonstrative multiphase flows, including turbulence-enhanced droplet atomization and multiple droplet control in the Stokes limit.

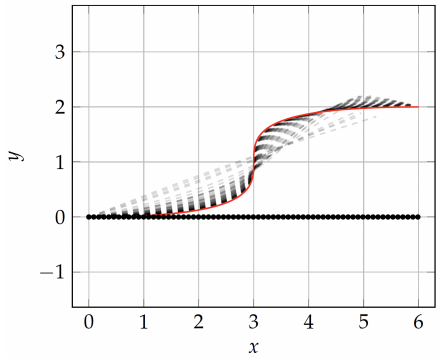

FIGURE 1. *Desired trajectory (red) in the $z = 0$ plane of an initially spherical droplet. Suboptimal trajectories are shown as dashed lines.*

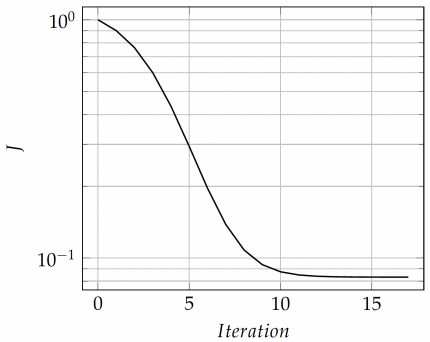

FIGURE 2. *Decrease of objective function Eq. (1) with adjoint-based gradient descent.*

References

[1] L. Vu, A. Fikl, D. J. Bodony, and O. Desjardins. Adjoint-based optimal control of an air-blasted planar sheet. Presented at the ILASS-Americas 30th Annual Conference on Liquid Atomization and Spray Systems, Tempe, AZ, May 2019.
[2] A. Fikl and D. J. Bodony. Adjoint-based interfacial control of axisymmetric viscous drops. Presented at the ILASS-Americas 30th Annual Conference on Liquid Atomization and Spray Systems, Tempe, AZ, May 2019.
[3] A. Fikl and D. J. Bodony. Jump relations of certain hypersingular Stokes kernels on regular surfaces. *SIAM J. Appl. Math.*, 80(5):2226–2248, 2020.
[4] A. Fikl and D. J. Bodony. Adjoint-based interfacial control of viscous drops. *Journal of Fluid Mechanics*, 911(A39), March 2021.

ADJOINT-BASED OPTIMISATION OF INTERFACIAL FLOWS IN THE SHARP INTERFACE LIMIT

Tomas Fullana[1], Alejandro Quirós Rodríguez[1], Vincent Le Chenadec[2], Taraneh Sayadi[1]
[1]*Sorbonne Université, Institut Jean le Rond d'Alembert, IJLRA, F-75005 Paris, France*
[2]*MSME, Univ Gustave Eiffel, UPEC, CNRS, F-77454 Marne-la-Vallée, France*

The flows encountered in energy conversion systems consist of a wealth of complex phenomena, including interfaces, reactions and turbulence. While the past decades have seen remarkable progress in computing capabilities, allowing computational fluid dynamics to become an ever more present tool in describing and predicting such multi-physics flows, these state-of-the-art computational resources still provide limited insight towards a robust optimization framework for technological applications. Targeted manipulation of such flows by enhanced designs or active control strategies is indeed crucial for improvements in performance and robustness and venturing beyond standard operating conditions. The transition from model-based numerical simulations to model-based optimal control requires an alternative approach, which allows access to inverse information. In the fields of external aero-dynamics and aero-acoustics for example, the introduction of such an approach has led to improved airframe designs and reduced noise production levels, with considerable economical, environmental and health-related implications.

The multi-physics aspects of interfacial two-phase flows however constitute a far larger step in complexity, due to the presence of discontinuities across the interface, and to the highly unsteady nature of the flow. As far as two-phase flows are concerned, to date, inverse information has been extracted from simulations of simplified configurations with additional unrealistic assumptions, or from low-fidelity models.

In this work, gradient based optimisation is performed on a Stefan problem, where the motion of the interface is a function of the jump in the temperature gradient. In particular, we study the growth or retraction of crystal shapes by taking into account the curvature effects at the boundary (Figure 1). In order to capture the movement of the interface, the one-fluid formulation is used, where the sharp interface is represented using a level set method. The gradient is extracted using an adjoint-based formulation and specifically defined tracking-type objective functions are minimized to control the final shape of the crystal.

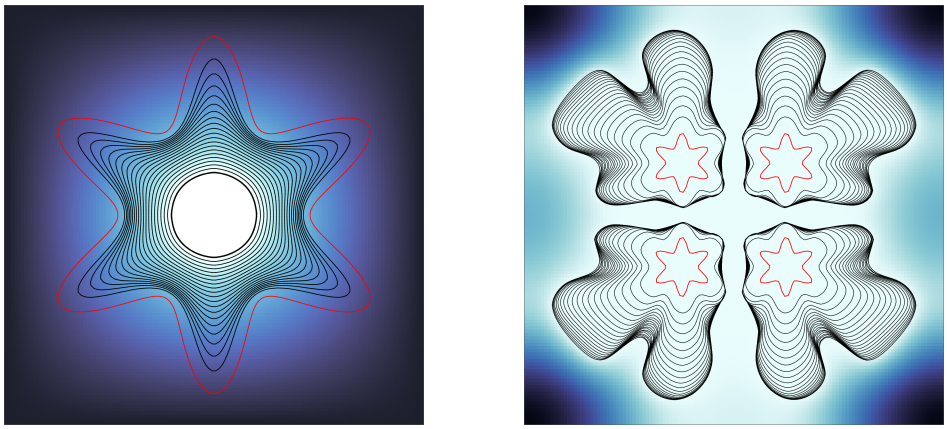

FIGURE 1. *The red curves represent the initial shape of the interface and the black ones the interface as time advances. Left : retraction of an ice crystal towards a circular shape in a liquid bath. Right : growth of four crystals in an undercooled liquid.*

GLOBAL RECEPTIVITY ANALYSIS: TOWARD PHYSICALLY REALIZABLE DISTURBANCES IN HYPERSONIC BOUNDARY LAYERS

Omar Kamal[1], Matthew T. Lakebrink[2], Tim Colonius[1]
[1] *California Institute of Technology, 1200 E. California Blvd., Pasadena, CA 91125, USA (okamal@caltech.edu)*
[2] *The Boeing Company, 325 James S. McDonnell Blvd., Hazelwood, MO 63042, USA*

Global resolvent or input/output analysis has become a popular method for analyzing worst-case disturbances in boundary layers. This framework relies upon maximizing an output quantity, usually the total energy of the disturbances, by determining an optimal global forcing. Although these existing input/output analyses have been previously applied to boundary layers [1, 2], there has not, to our knowledge, been an attempt to constrain the optimization problem to physically realizable inputs, i.e. freestream disturbances in the form of incident acoustic, vortical, and entropic waves.

In this work, we address the global natural receptivity problem by embedding the scattering-wave theory into global input/output analysis to determine worst-case disturbances from freestream acoustic or vortical/entropic waves. We employ both global resolvent analysis and the computationally efficient, parabolized One-Way Navier-Stokes technique [5] to study the natural receptivity of hypersonic boundary layers and compare to the unconstrained forcing problem.

We first apply our optimal scattering-wave framework to a 2D Mach 4.5 adiabatic-wall, flat-plate boundary layer, where the input is restricted to freestream fast acoustic waves, and plot the optimal inputs and responses in Fig. 1. The transmitted acoustic waves near the leading edge undergo diffraction and diffusion, with its streamwise component exhibiting strong resonant interactions with Mode I waves [3]. These waves synchronize with the first mode at $x^* \approx 0.0766$ m, giving rise to the second mode. The input fields reveal most of the energy to be concentrated at the leading edge where the highest base-flow nonparallelism is present, and thus the most efficient mechanism to convert freestream disturbance energy into instability modes [4].

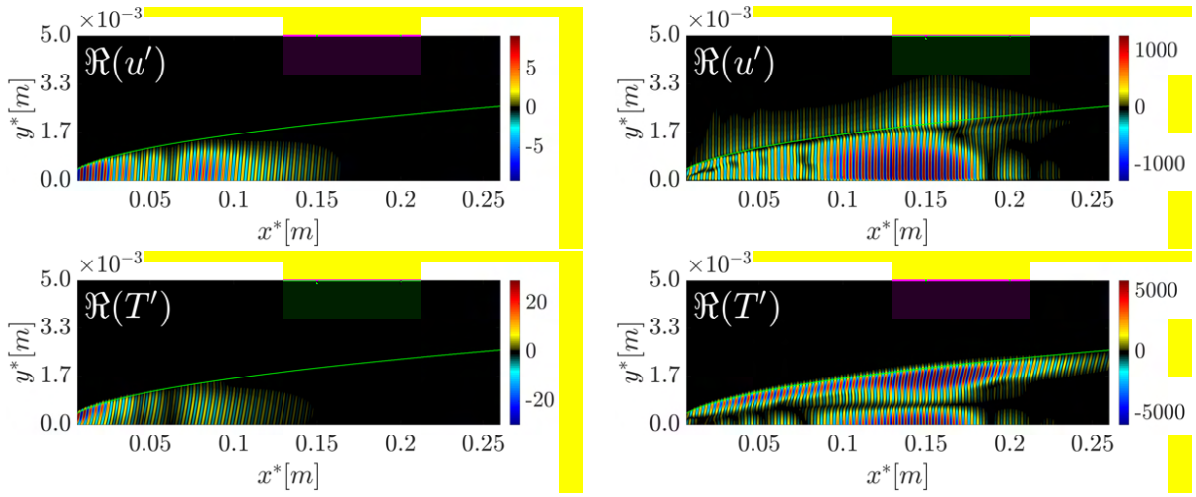

Figure 1: Optimal u' and T' inputs (left) and responses (right) with freestream fast acoustic waves at $F = \frac{\omega^* \nu^*_\infty}{U^{2*}_\infty} = 2.2 \times 10^{-4}$. The green contour represents the boundary-layer edge ($\delta = 0.99 U_\infty$).

After thorough validation, we plan to apply this technique on more complex geometries to illuminate the intricate receptivity mechanisms present under realistic flight conditions. This novel methodology can serve as an efficient, modern tool for studying natural receptivity of boundary layers.

References

[1] B. Bugeat, J.-C. Chassaing, J.-C. Robinet, and P. Sagaut. 3d global optimal forcing and response of the supersonic boundary layer. *Journal of Computational Physics*, 398:108888, 2019.
[2] D. A. Cook and J. W. Nichols. Free-stream receptivity of a hypersonic blunt cone using input–output analysis and a shock-kinematic boundary condition. *Theoretical and Computational Fluid Dynamics*, 2022.
[3] Y. Ma and X. Zhong. Receptivity of a supersonic boundary layer over a flat plate. part 2. receptivity to free-stream sound. *Journal of Fluid Mechanics*, 488:79–121, 2003.
[4] W. S. Saric, H. L. Reed, and E. J. Kerschen. Boundary-layer receptivity to freestream disturbances. *Annual review of fluid mechanics*, 34(1):291–319, 2002.
[5] A. Towne and T. Colonius. One-way spatial integration of hyperbolic equations. *Journal of Computational Physics*, 300:844–861, 2015.

LINEAR SENSITIVITY OF A HYPERSONIC BOUNDARY LAYER BY ALGORITHMIC DIFFERENTIATION THROUGH THE CFD TOOLBOX *BROADCAST*

Arthur Poulain[1], Cédric Content[1], Denis Sipp[1], Georgios Rigas[2], Eric Garnier[1]
[1]*DAAA, ONERA, Université Paris Saclay, F-92190 Meudon, France - arthur.poulain@onera.fr*
[2]*Imperial College London, South Kensington, London, United Kingdom*

The evolution of any complex dynamical system is described by the derivative operators. However the extraction of the exact N-order derivative operators is often inaccurate and requires approximations from the user. The open-source CFD code called BROADCAST discretises the laminar compressible Navier-Stokes equations and then linearises the exact N-derivative operators through Algorithmic Differentiation (AD) providing a toolbox for laminar flow dynamic analyses. Furthermore, the gradients through adjoint derivation are extracted straightly by transposition of the linearised operator. The software includes baseflow computation, linear global stability and sensitivity tools. Numerical method consists in a finite-difference high-order shock-capturing scheme [1] applied in a finite volume framework on 2D curvilinear structured grids. Application of the code is made on the linear stability of a hypersonic laminar boundary layer at $M = 4.5$ through the following steps. First, a 2D baseflow, initialised by a compressible self-similar solution, is computed by a Newton method. Extraction of the Jacobian operator is made by matrix-vector products produced by Algorithmic Differentiation with the software TAPENADE [2]. Then, 2D global stability through resolvent operator is performed highlighting the second Mack mode. Extension towards 3D periodic instability analysis through AD is offered and underlines the streaks and first Mack mode. The optimal forcing and response have very similar shape to those obtained by Bugeat [3] however the optimal gain at high frequency converges at a lower computation cost thanks to the high-order scheme with lower dissipation. Then, the evolution of the optimal gain resulting from the resolvent problem is computed with the Hessian operator [4]. Starting from the sensitivity to basefow modification, the sensitivity with respect to wall-boundary condition parameters can be derived [5]. Small variations of wall-temperature and wall-normal blowing are for instance considered on the 2D second Mack mode optimal gain. The general result from Mack that wall cooling destabilises the second mode [6] is thus recovered but in addition the profile of optimal wall-cooling is straightforwardly computed (Figure 1). This represents a first step towards quick design of open-loop control devices.

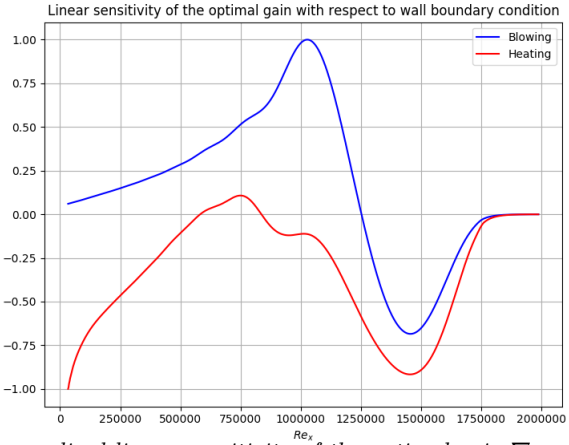

FIGURE 1. *Evolution of the normalised linear sensitivity of the optimal gain $\nabla_{BC}\mu^2$ to wall boundary conditions (heating or blowing) with respect to the Reynolds number based on x for the 2D second Mack mode.*

References

[1] L. Sciacovelli, D. Passiatore, P. Cinnella and G. Pascazio. Assessment of a high-order shock-capturing central-difference scheme for hypersonic turbulent flow simulations. *Computers and Fluids*, 2021.
[2] L. Hascoët and V. Pascual. The Tapenade Automatic Differentiation tool: Principles, Model, and Specification. *ACM Transactions On Mathematical Software*, 2013.
[3] B. Bugeat, J.-C. Chassaing, J.-C. Robinet, and P. Sagaut. 3D global optimal forcing and response of the supersonic boundary layer. *Journal of Computational Physics*, 2019.
[4] C. Mettot, F. Renac and D. Sipp. Computation of eigenvalue sensitivity to base flow modifications in a discrete framework: Application to open-loop control. *Journal of Computational Physics*, 2014.
[5] A. Martínez-Cava Aguilar. Direct and adjoint methods for highly detached flows. *Espacio*, 2019.
[6] L. Mack. Effect of cooling on boundary-layer stability at Mach number 3. *Instabilities and Turbulence in Engineering Flows*, 1993.

STUDIES OF DISTURBANCE GROWTH IN TRANSONIC BOUNDARY LAYERS OVER COMPLEX GEOMETRIES USING EMBEDDED DG SIMULATIONS

Ganlin Lyu[1], Chao Chen[2], Shahid Mughal[1], Xi Du[2], Spencer J. Sherwin[1]
[1] *Imperial College London, United Kingdom*
[2] *Beijing Aircraft Technology Research Institute of COMAC, Beijing, 102211, China,*

Laminar boundary layer natural transition for external flows is of particular interest in both the aeronautical industry and academia. The transitional process is dominated by the linear growth of disturbances, e.g., Tollmien–Schlichting waves and crossflow waves, and therefore a correct prediction on the development of the disturbances is necessary for a successful transitional analysis. Most conventional studies focused on the disturbances developing based on incompressible boundary layer flows over ideal, clean geometries. However, the physical settings for the real conditions are different for the flow compressibility and geometrical complexity. The compressibility stems from the transonic operational conditions, and for the real geometries the main source of the complexity is the existence of surface imperfections, which typically take the form of steps and gaps whose sizes are comparable with the boundary layer thickness. In the current work we therefore further extend the physical settings to transonic laminar boundary layer at realistic Reynolds numbers, and over wing sections with surface imperfections. Our study will utilize the solver in the spectral/hp element framework Nektar++ [1], where the high-order features enable accurate boundary layer profile computations over complex geometries (which may well include locally reversed flows), as well as the ability to capture disturbance development with high accuracy and higher fidelity in physics. The validation and correctness of the method will be demonstrated by analyzing a two-dimensional transonic flow over flat plates at Mach 0.8. Both clean geometry and the geometry with a forward-facing step are studied. The zero-pressure gradient is adopted for the clean case while for the stepped case pressure gradient is generated due to the existence of the step although the same boundary conditions are enforced. The N-factors are generated in the Rex range from 0.5E6 to 4.0E6. Figure 1(a) shows that a good agreement in the comparison of the N-factor obtained by others verifies the approach. Moreover, it is worth mentioning that the reflected wave at the step, as is given in Figure 1(b), is dominated by acoustics since the pressure component has the largest amplitude while the velocity components also have a comparable amplitude. We then study the disturbance development over wing sections with surface imperfections. High fidelity DG simulations are carried out in a near-wall, reduced domain which is embedded in a full three-dimensional RANS solution. The boundary data of the reduced domain is interpolated from the outer solution, and pressure compatibility is achieved through the entropy-pressure compatible Riemann inflow [2]. After the computation for the disturbance fields, the N-factor on this wing section is subsequently generated. In the conference we will demonstrate the simulation results of the disturbances' growth with the existence of a step as well as cover the following analysis.

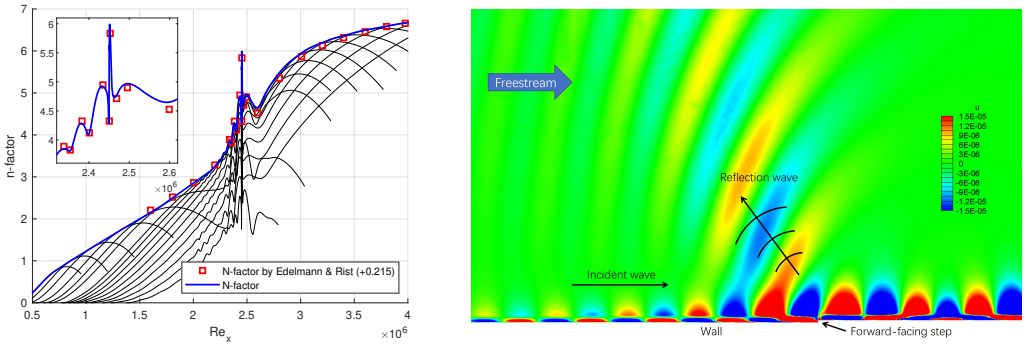

(a) N-factor comparison (b) Wave reflection at the step

FIGURE 1. *Tollmien-Schlichting wave development over a flat plate with a forward-facing step.*

References

[1] C.D. Cantwell, D. Moxey, A. Comerford, et al. Nektar++: An Open-source Spectral/hp Element Famework. *Computer Physics Communications*, 192:205–219, 2015.
[2] G. Lyu, C. Chen, X. Du, S.J. Sherwin. Pressure-density compatible Riemann boundary condition for DG compressible flow simulations. *International Conference on Spectral and High Order methods (ICOSAHOM 2020)*, 2021.

THEORETICAL AND EXPERIMENTAL STUDY OF TRANSITION IN CHOKED NOZZLES

Zebrowski, B.[1], Jordan, P.[1], Jaunet, V.[1], Martini, E.[1]
[1]*Institut Pprime - UPR 3346, CNRS-ENSMA-Université de Poitiers, Département Fluides, Thermique et Combustion, 86360 Futuroscope-Chasseneuil, France*

In this work, we study the laminar to turbulent transition of boundary layers in converging-diverging nozzles used as standard gas flow meters. The aim is to characterize the transition using the stability theory framework and compare the predicted trends in an experimental investigation.

Experimental measurements are carried out in a controlled environment where we investigate the sensitivity of transition to wall roughness, freestream turbulence and nozzle throat radius of curvature. The transition is detected through temperature change in adiabatic wall recovery temperature [1]. An example of infrared measurement is shown in Figure 1. Laminar boundary layers are obtained using an analytic formulation for nozzles [2], including compressibility and favourable pressure gradient. Stability characteristics are addressed using the linear stability framework under the parallel flow assumption. We show that the usually unstable Tollmien-Schlichting wave is stabilized by the pressure gradient and that the flow is stable to modal disturbances. A parabolic approach is then employed to perform a spatial transient growth study [3]. We show that the boundary layer can experience significant transient energy growth in the form of streamwise streaks. The peak of transient energy is found to scale with Re^2 and to be located at a constant distance of half the throat diameter, independently of upstream stagnation condition and nozzle wall curvature.

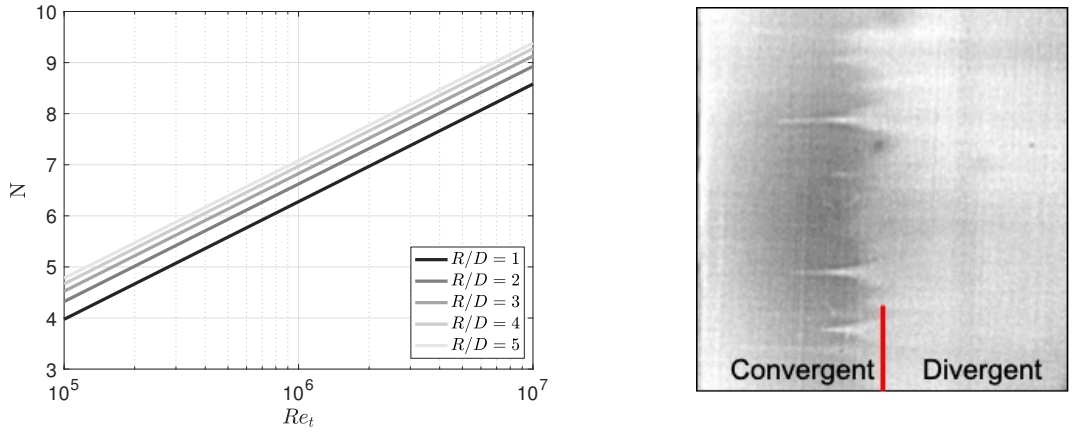

Figure 1: Left: Evolution of N factor with throat based Reynolds number (Re_t) for multiple nozzle wall radius. Right: infrared image of planar nozzle wall. Flow is from left to right. The red line indicates the throat location. The sudden variation in gray shade at nozzle throat indicate the transition from laminar to turbulent. The elongated streamwise structures are transition spots induced by isolated roughness elements.

An e^N criterion is used to predict the transition Reynolds number. N factors are computed for various nozzle wall radius and Reynolds numbers. The results presented in Figure 1 show that increasing the throat radius of curvature is destabilizing the boundary layer, complying with previous experimental observations [4]. In our experiment, the various freestream turbulence levels are characterized with hotwire measurements that allow direct comparison with the transition trend predicted by the stability theory. We also show that, below a critical wall roughness, the transition is dominated by incoming freestream disturbances.

References

[1] C. Tropea, A. Yarin and J. Foss. *Springer Handbook of Experimental Fluid Mechanics*. Springer, Chicago, USA, 2007.
[2] D. Geropp. Laminare grenzschichten in ebenen und rotationssymmetrischen lavaldsen. In *Deutsche Luft- und Raumfahrt*; 71-90, 1971.
[3] A. Tumin and E. Reshotko. Spatial theory of optimal disturbances in boundary layers. *Phys. of Fluids*, 13, 2001.
[4] M. Ishibashi. Discharge coefficient equation for critical-flow toroidal-throat venturi nozzles covering the boundary-layer transition regime. *Flow Measur. and Instrum.*, 44:107-121, 2015.

LINEAR AND NON-LINEAR DYNAMICS OF HYPERSONIC BOUNDARY LAYER STREAK INSTABILITIES

Clément Caillaud[1,3], Guillaume Lehnasch[1], Peter Jordan[2], Eduardo Martini[1,3], Eric Goncalves[1], Ludovic Hallo[3], Thibault Bridel[3]
[1] *Institut Pprime - ISAE-ENSMA, contact : clement.caillaud@isae-ensma.fr,*
[2] *Institut Pprime - CNRS*
[3] *CEA-CESTA*

Hypersonic boundary layer receptivity and transition to turbulence is tightly linked to the emergence of longitudinal steady streaks for realistic conditions [3]. These vortical structures stem from various sources such as surface roughness, parametric modes interactions or curvature. The emerging streaks then lead to a distorted base flow inducing secondary instability and interactions with the existing modes of the canonical boundary layer [1]. While the linear evolution of selected streaks modes in hypersonic cone boundary layer has been recently described [2], the full transition route from receptivity to non-linear breakdown has not been detailed.

This study aims to explore the differences between linear and non-linear dynamics of streaks instability at high speeds under broadband forcing. Mach 6 boundary layers with streaky structures were constructed on a flat plate using a DNS forced at the inflow with the optimal forcing obtained from local linear stability analysis. Different streak amplitudes were considered. A white noise forcing is propagated with a linear and a non-linear DNS and the various growing modes are tracked. The linear and non-linear responses of the streaky base flows, such as in Fig. 1, are decomposed in frequency-wavenumber space through spanwise Floquet analysis and SPOD. Modes emerging from the white noise forcing, and their downstream evolution as streaks grow in amplitude, are compared to modes of evolution obtained from the spatial 2D-linear stability problem (Fig. 2). Transition scenarios under broadband forcing are discussed. Our results show an early dominance of sub-harmonic oblique streak modes, even for low amplitude streaks. Furthermore, distorted Mack modes of weaker amplification are also found, with two distinct frequencies. These results suggest that even at low amplitude, streaks can substantially change the transition route from the usual second mode dominated Blasius boundary layer.

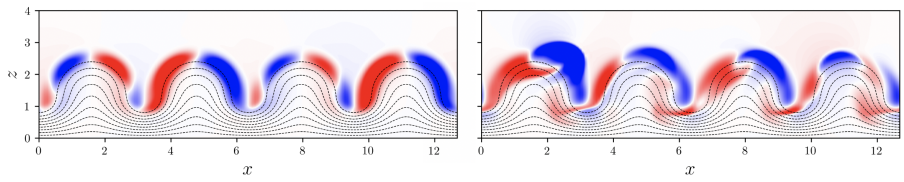

FIGURE 1. *Disturbance fields at the end of the domain ($x = 350\delta_0$). Dashed lines: base flow velocity ; contours : axial velocity disturbances from the linear (left) and non-linear (right) DNS*

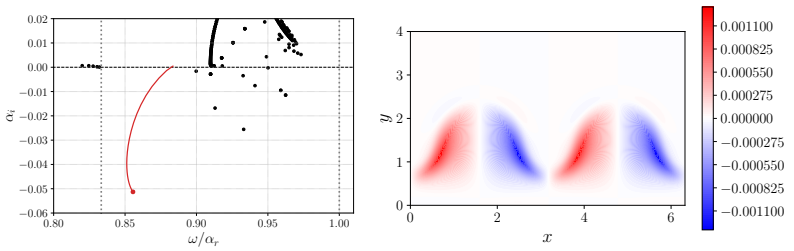

FIGURE 2. *Left : spatial spectrum at $x = 350\delta_0$ for $f = 0.56$ with locus of the most amplified mode (red) as streaks amplitude increases. Right : contours of axial velocity for the corresponding most amplified mode.*

References

[1] P. ANDERSSON, L. BRANDT, A. BOTTARO, AND D. S. HENNINGSON, *On the breakdown of boundary layer streaks*, 428, pp. 29–60.
[2] P. PAREDES, M. M. CHOUDHARI, AND F. LI, *Instability wave–streak interactions in a high Mach number boundary layer at flight conditions*, 858, pp. 474–499.
[3] K. STETSON, *Nosetip bluntness effects on cone frustum boundary layer transition in hypersonic flow*, in 16th Fluid and Plasmadynamics Conference, American Institute of Aeronautics and Astronautics.

COMPRESSIBILITY EFFECTS ON THREE-DIMENSIONAL SECONDARY INSTABILITIES IN THE CYLINDER PERIODIC WAKE

L-Victoria Rolandi[1], Jérôme Fontane[1], Jérémie Gressier[1], Thierry Jardin[1] and Laurent Joly[1]
[1]*ISAE-SUPAERO, Université de Toulouse, 31400 Toulouse, France*

With a growing interest in low Reynolds numbers compressible flows, the aim of this work is to investigate compressibility effects on the wake dynamics of the circular cylinder. In particular, our focus is made on the so called Mode A and Mode B secondary instabilities, which are responsible of the transition from a two-dimensional periodic to a three-dimensional state [1, 2]. Mode A appears at $Re \approx 180 - 190$ and is associated with an elliptic instability of the primary vortex cores with large scale transverse structures at a spanwise wavelength of $\lambda_z \sim 4D$, where D indicates the cylinder diameter. Mode B, which arises at $Re \approx 230 - 260$, is instead associated with a hyperbolic instability developing in the braid region and is related to the formation of finer scale structures of characteristic wavelength $\lambda_z \sim 1D$.
We address the influence of compressibility on these modes. The analysis has been conducted for Reynolds numbers $Re \in [200; 350]$ and Mach numbers up to $M_\infty = 0.5$. The two-dimensional periodic base state is found to exhibit time-averaged properties that substantially vary within the range of Reynolds and Mach numbers considered. Specifically, three different types of time-averaged flow structure are identified when varying both Reynolds and Mach numbers, as shown in Fig. 1 for three representative cases.

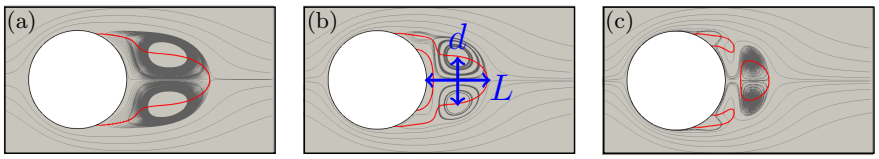

FIGURE 1. *Time-averaged base flow structures: a) Type 1, b) Type 2 and characteristic length scales, c) Type 3. Streamlines are shown in gray color and the time averaged longitudinal velocity isocontour $\bar{u}_x = 0$ is shown in red.*

The two-dimensional periodic flow is used as base state for a global stability analysis performed by means of Floquet theory. The global modal stability solver [3] is based on the Krylov–Schur algorithm with a time-stepping approach. A stabilizing (decreasing Floquet multiplier μ) or a destabilizing (increasing μ) effect of compressibility is observed on Mode A depending on the Reynolds number and the mode wavelength, while Mode B is found to be stabilized by compressibility (see Fig. 2). Interestingly, the

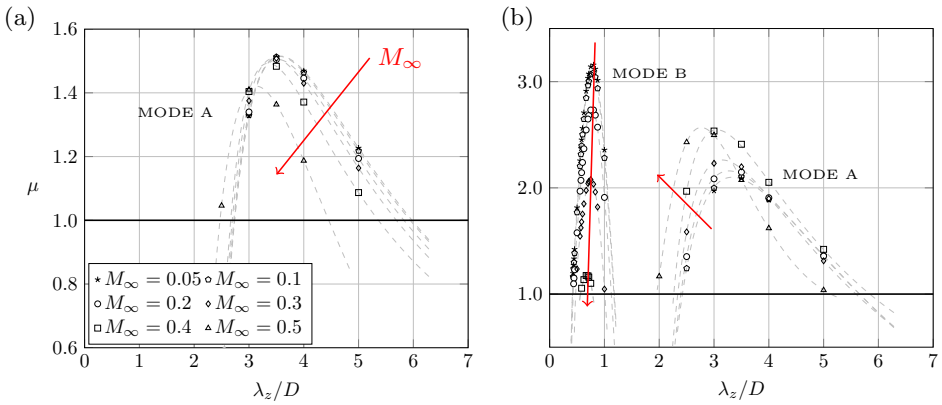

FIGURE 2. *Floquet multiplier μ as a function of the spanwise wavelength λ_z at (a) $Re = 250$ and (b)$Re = 350$ for different Mach numbers. Dashed lines represent the interpolation curves for a given Mach number.*

characteristic length-scales of the time-averaged base flow recirculation region (highlighted in Fig. 1.b) are found to be relevant for the normalisation of the instability wavelengths λ_z. The Mach number increase is also found to promote vorticity anisotropy on Mode A at largest wavelengths, which is not instead observed for Mode B.

References

[1] D. Barkley and R.D. Henderson. Three-dimensional Floquet stability analysis of the wake of a circular cylinder. Journal of Fluid Mechanics, 322, 215–241, 1996,
[2] J.S. Leontini, D. Lo Jacono and M.C. Thompson. Stability analysis of the elliptic cylinder wake Journal of Fluid Mechanics,763,302–321,2015.
[3] L.V Rolandi, T. Jardin, J. Fontane, J. Gressier and L. Joly. Stability of the low Reynolds number compressible flow past a NACA0012 airfoil. AIAA Journal,1–15,2021.

First name	Surname	Affiliation	E-mail
Alberto Felipe	Rius Vidales	Delft University of Technology	A.F.RiusVidales@tudelft.nl
Alejandro	Quirós Rodríguez	Sorbonne University	alejandro.quiros_rodriguez@etu.sorbonne-universite.fr
Aliza	Abraham	CNRS-IRPHE, Aix-Marseille Université	aliza.ABRAHAM@univ-amu.fr
Antoine	Jouin	DynFluid Laboratory, ENSAM	antoine.jouin@ensam.eu
Anton	Glazkov	KAUST	anton.glazkov@gmail.com
Ardeshir	Hanifi	KTH Royal Institute of Technology	hanifi@kth.se
Arthur	Poulain	DAAA, ONERA, Université Paris Saclay	arthur.poulain@onera.fr
Athanasios	Margaritis	Imperial College London	a.margaritis@imperial.ac.uk
Bruno	Zebrowski	Institut Pprime / CEA-CESTA	bruno.zebrowski@ensma.fr
Clément	Caillaud	Institut Pprime / CEA-CESTA	clement.caillaud@isae-ensma.fr
Dan	Henningson	KTH Royal Institute of Technology	henning@kth.se
Daniel	Bodony	University of Illinois at Urbana-Champaign	bodony@illinois.edu
David	Fabre	IMFT Universiy of Toulouse	david.fabre@toulouse-inp.fr
Diego	Bonkowski Sierra Audiffred	Instituto Tecnológico de Aeronáutica	diegodbsa@ita.br
Diego	C. P. Blanco	Instituto Tecnológico de Aeronáutica	diegodcpb@ita.br
Eduardo	Martini	Institut Pprime / CEA-CESTA	eduardo.martini@univ-poitiers.fr
Flavio	Giannetti	University of Salerno	fgiannetti@unisa.it
Francesco	Tocci	DLR	francesco.tocci@dlr.de
Francesco	Scarano	ISAE – Supaero	francesco.scarano@isae-supaero.fr
Francios	Gallaire	École polytechnique fédérale de Lausanne	francois.gallaire@epfl.ch
Gabriele	Nastro	Laboratoire PRISME, Université d'Orléans	gabriele.nastro@univ-orleans.fr
Ganlin	Lyu	Imperial College London	g.lyu19@imperial.ac.uk
Georgios	Rigas	Imperial College London	g.rigas@imperial.ac.uk
Javier	Sierra Ausin	IMFT-UNISA	javier.sierra@imft.fr
Jeac-Christophe	Robinet	Arts et Métiers DynFluid Lab.	Jean-Christophe.Robinet@ensam.eu
Jens	Fransson	KTH Royal Institute of Technology	jensf@kth.se
Jitong	Ding	University of Melbourne	jitongd@student.unimelb.edu.au
Jordi	Casacuberta	Delft University of Technology	J.CasacubertaPuig@tudelft.nl
José	Faúndez Alarcón	KTH Royal Institute of Technology	josfa@kth.se
José Ignacio	Jiménez-González	Universidad de Jaén	jignacio@ujaen.es
Juan Alberto	Franco	DLR	juan.franco@dlr.de
Juan Ángel	Tendero Ventanas	Universidad de Cádiz	juanangel.tendero@uca.es
Julio	Soria	Monash University	julio.soria@monash.edu
Laura Victoria	Rolandi	ISAE-Supaero	laura-victoria.rolandi@isae-supaero.fr
Lutz	Lesshafft	LadHyX / Ecole Polytechnique	lesshafft@ladhyx.polytechnique.fr
Manuel	Lorite-Díez	Universidad de Granada	mldiez@ugr.es
Marina	Barahona	Delft University of Technology	M.BarahonaLopez@student.tudelft.nl
Marios	Kostinos	Delft University of Technology	m.kotsonis@tudelft.nl
Miguel	Beneitez	DAMTP, University of Cambridge	mb2467@cam.ac.uk
Miguel	Fosas	Universidad de Cádiz	miguel.fosas@uca.es
Omar	Kamal	California Institute of Technology	okamal@caltech.edu
Paolo	Luchini	Univ. Salerno	luchini@unisa.it
Pedro	Paredes	National Institute of Aerospace	pedro.paredes@nianet.org
Peter	Schmid	KAUST	peter.schmid@kaust.edu.sa
Ricardo	Frantz	DynFluid Laboratory, ENSAM	ricardo.frantz@ensam.eu
Simon	Kern	KTH Royal Institute of Technology	skern@kth.se
Soledad	Le Clainche	Universidad Politécnica de Madrid	soledad.leclainche@upm.es
Stefan	Hein	DLR	stefan.hein@dlr.de
Sven	Westerbeek	Delft University of Technology	s.h.j.westerbeek@tudelft.nl
Taraneh	Sayadi	Sorbonne University	taraneh.sayadi@sorbonne-universite.fr
Thomas	Jaroslawski	ONERA, Toulouse, France	thomas.jaroslawski@onera.fr
Tobias	Bölle	DLR	tobias.boelle@dlr.de
Tomas	Fullana	Sorbonne University	tomas.fullana@sorbonne-universite.fr
Tomas	Leweke	CNRS-IRPHE, Aix-Marseille Université	thomas.leweke@cnrs.fr
Tristan M.	Römer	University of Stuttgart	roemer@iag.uni-stuttgart.de
Ulrich	Rist	University of Stuttgart	rist@iag.uni-stuttgart.de
Valerio	Lupi	KTH Royal Institute of Technology	lupi@mech.kth.se
Vishal	Chaugule	Monash University LTRAC	vishal.chaugule@monash.edu
Yongxiang	Wu	University of Stuttgart	yongxiang.wu@iag.uni-stuttgart.de
Yves-Marie	Ducimetière	École Polytechnique Fédérale de Lausanne	yves-marie.ducimetiere@epfl.ch